AN ABSTRACT OF THE THESIS OF

Sang-Bin Park for the degree of Master of Science in Industrial Engineering presented on September 23, 1999. Title: The Use of Electrochemical Micromachining for Making a Microfloat Valve.

Redacted for Privacy

Abstract approved: _____

Brian K. Paul

Micromanufacturing consists of processes for producing structures, devices or systems with feature sizes measured in micrometers. Micromanufacturing began in the mid-1960's with microelectronics fabrication technology. In the 1980's, Micro-Electro-Mechanical Systems (MEMS) began to be developed, in which electrical and mechanical subsystems were integrated at small scales. More recently, Microtechnology-based Energy and Chemical Systems (MECS) have been developed that have led to improved heat and mass transfer in energy and chemical systems.

At Oregon State University, new methods to fabricate MECS have been developed. One of the new methods involves microlamination--bonding thin strips of different materials together. This method has generated a high volume and low-cost approach to the production of high-aspect-ratio (height-to-width) structures.

Past efforts to make microfloat valves using microlamination methods resulted in an 11:1 diodicity ratio. It was hypothesized that the valve had a ridge of redeposited material around the valve seat caused by the condensation and deposition of ablation ejecta during laser machining.

The contribution of this thesis is the creation of a microfloat valve using an Electrochemical Micromachining (EMM) method. EMM methods are known to produce smooth surfaces, free of burrs or any other types of aspirates. Therefore, it was hypothesized that float valves made with EMM methods would improve valve performance.

Four steps were involved in the creation of the microfloat valve: lamina formation, laminae registration, laminae bonding and component dissociation. A total of 9 laminae-some of which were made with 304 stainless steel 76.2 μm thick, others of which were made with 50.8 μm thick polyimide-made up the microfloat valve. Photolithography and EMM were used to form the lamina. Even though the laminae created by EMM were smaller in size than desired, the machined areas did not have redeposited material, and some areas had straight walls.

In laminae registration, a two edge registration method was used. In the laminae bonding step, laminae were bonded by the adhesive method at 248°C under 135 kPa pressure for 13.5 minutes. In the component dissociation step, a capacitor dissociation method that was designed at OSU was used.

Upon performance testing, the average diodicity ratio for the EMM valve was 12.45 over the range 0 kPa-450 kPa, indicating improved performance when compared to the Laser Ablation valve- which had an average 11.17 over the range 0 kPa-100 kPa. Microscope examination of valves revealed that statistically significant improvement in valve performance would require refinement of component dissociation methods.

The Use of Electrochemical Micromachining for Making a Microfloat Valve

by

Sang-Bin Park

A THESIS

Submitted to

Oregon State University

in partial fulfillment of
the requirements for the
degree of

Master of Science

Presented September 23, 1999
Commencement June 2000

Master of Science thesis of Sang-Bin Park presented on September 23, 1999

APPROVED:

Redacted for Privacy

Major Professor, representing Industrial Engineering

Redacted for Privacy

Head of Department of Industrial and Manufacturing Engineering

Redacted for Privacy

Dean of Graduate School

I understand that my thesis will become part of the permanent collection of Oregon State University libraries. My signature below authorizes release of my thesis to any reader upon request.

Redacted for Privacy

Sang-Bin Park, Author

ACKNOWLEDGEMENTS

This thesis was made possible through the effort and support of many people, so I would like to thank all of them. First, I would like to thank Dr. Brian K. Paul, who is my advisor. His advice and support enabled me to finish this thesis. I would also like to thank Dr. Rick Wilson, Dr. Kimberly Douglas, Dr. Dean Jensen and Dr. Darius Adams for being my committee members, and Dr. Deborah Pence for her help.

The EMM portion of this thesis was supported by and carried out at Pacific Northwest National Laboratories during the summer, 1998. I wish to express my particular appreciation to Dr. Peter Martin, Dr. Dean Matson, Wendy Bennett, Charles Bonham, Donald Stewart, John Johnston, and David Lettau for their support. My experience at PNNL will be very valuable to me throughout my life.

There are many friends who helped me finish this thesis. In my department, I would like to thank Steve Etringer, Kannachai Kanlayasiri, Michael Gabriel, Jianping Wen, Wassanai Wattanutchariya, Worawut Wangwatcharakulsites, Tyson Terhaar, and Tyler Dewey. I also extend my appreciation to Seung-Ho Yu and Bong-Im Jeon.

I would like to thank Juliana Coons for her advice on my writing skills. Also, I wish to thank my family for their support and prayers while I study abroad. Finally, I want to thank my wife for her loving care and encouragement.

Finally, thanks to God for leading me to stand here.

TABLE OF CONTENTS

TABLE OF CONTENTS (Continued)

LIST OF FIGURES

Figures **Page**

LIST OF FIGURES (Continued)

Figure **Page**

LIST OF TABLES

LIST OF ABBREVIATIONS

MEMS	MicroElectroMechanical Systems
MECS	Microtechnology-based Energy and Chemical Systems
OSU	Oregon State University
EMM	Electrochemical Micromachining
ECM	Electrochemical Machining
UV	Ultra Violet
PNNL	Pacific Northwest National Labs
SSW	Solid-State Welding
CIM	Computer-intergrated Manufacturing
CAD	Computer-aided Design
DI	Deionized
ESI	Electro Scientific Industries

The Use of Electrochemical Micromachining for Making a Microfloat Valve

1. INTRODUCTION

Micromanufacturing is the art of producing miniature systems. Micromanufacturing comprises processes for producing structures, devices or systems with feature sizes measured in micrometers.[1] Micromanufacturing began in the mid 1960's with microelectronics fabrication technology. Micro-Electro-Mechanical Systems (MEMS) began to be developed in 1980's, in which electrical and mechanical subsystems were integrated at small scales.[2] More recently, micromanufacturing techniques have been developed to fabricate Microtechnology-based Energy and Chemical Systems (MECS). MECS have the potential to improve heat mass transfer in energy and chemical systems.

Researchers at Oregon State University (OSU) are working to develop new methods to fabricate MECS. One new method involves microlamination, in which thin strips of material are formed and bonded together. By using microlamination methods, high volume, low-cost production of high-aspect-ratio (height-to-width) structures has been achieved.[3] Past methods of lamina forming have included laser and chemical micromachining. In this thesis, Electrochemical Micromachining (EMM) will be introduced as a new method for lamina forming for microlamination.

EMM applies Electrochemical Machining (ECM) to the forming of thin films. ECM uses a non-toxic electrolyte to remove metal while having a high machining rate, good process control and flexibility, and a wide range of electrically conductive materials. The workpiece and tool are held close together and an electrochemical reaction removes metal ions from the workpiece. An electrolyte flows through the gap between them and washes away the swarf.[4,5]

The objective of this thesis is to apply through-mask EMM to the fabrication of a microfloat valve. One researcher at OSU has already made a microflapper valve using a microlamination procedure involving laser micromachining and microprojection welding, and a microfloat valve using laser micromachining, microprojection welding and component dissociation.[6] The difference between a float valve and flapper valve is whether or not the valve is free-standing or attached (Figure 1). The disk of a float valve (Figure 1a) is

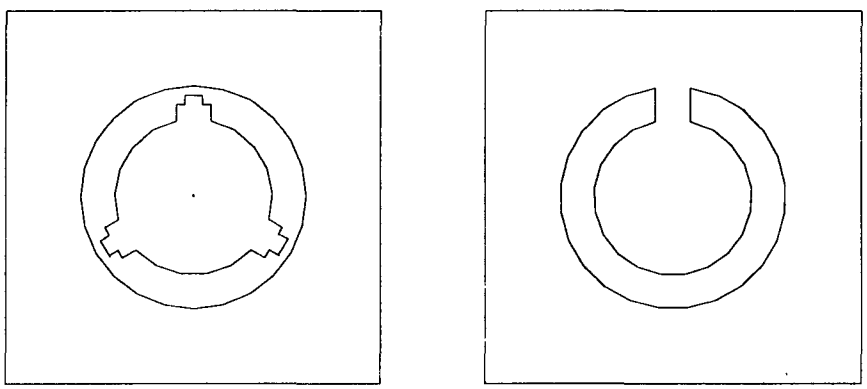

(a) A float valve (b) A flapper valve

Figure 1. Float Valve and Flapper Valve

detached and stands freely, moving up and down to allow fluids flow. The disk of a flapper valve (Figure 1b) is attached to the body of the valve, so that the disk to bends to open and close, controlling flow to allowing flow.

This study concentrated on the use of a microlamination procedure involving EMM and adhesive bonding to make a microfloat valve. Four steps were carried out to laminate a microfloat valve: 1) lamina forming, 2) laminae registration, 3) laminae bonding, and 4) component dissociation. The microfloat valve consisted of nine laminae (Figure 3). A substrate of 76.2 μm thick stainless steel was processed using photolithography to make Lamina 1, 3, 5, 7, and 9 during the lamina forming step. This was accomplished by exposing the substrate to Ultra Violet (UV) light through a Kapton mask. The mask was fabricated by laser machining.

Next, the EMM method was carried out to form laminae so that five different laminae were made to make a set of microfloat valves. Then, 50.8 μm thick polyimide was cut by laser machine to form Lamina 2,4,6, and 8. Through the use of a jig, the alignment of the nine laminae was registered, and then bonded using the adhesive bonding method. The third lamina has three fixture bridges which connect with a disk in its center and with its body. These three fixture bridges were dissociated by using the capacitor dissociation method developed at OSU.[6] The lamina forming step using stainless steel was carried out at Pacific Northwest National Laboratory (PNNL) because of non-availability of an EMM machine at OSU.

Past efforts to make a microfloat valve resulted in an 11:1 diodicity ratio. One reason for the limited diodicity of the valve is that a ridge of redeposited material around the valve nozzle is caused by the condensation and deposition of ablation ejects during the laser machining of laminates. An advantage of EMM is that it can form smooth surfaces free of burrs or any other types of aspirates. Therefore, it is expected that by applying EMM to the fabrication of microfloat valves, improvements in diodicity of the float valve will be made.

2. LITERATURE REVIEW

2.1 Electrochemical Machining (ECM)

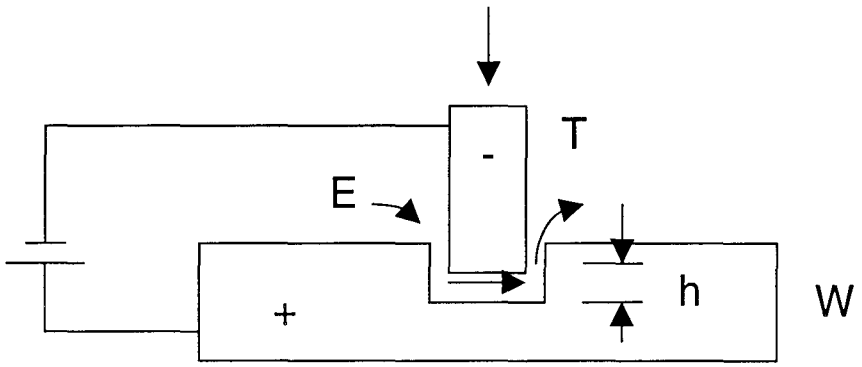

Figure 2. The ECM Method

Figure 2 shows the principle of the ECM method for making a cavity with a rectangular cross-section. An electrolyte (E) pumped at high pressure flows through the gap (h) between the tool (T) and the workpiece (W). A voltage is applied between the workpiece (anode) and the tool (cathode), which produces an electric current. Therefore, a local dissolution of the metal, M, of the anode is generated by the reaction:

$$M \rightarrow M^{n+} + n\,e$$

where n^+ is the charge of the metal ion produced. Meanwhile, at the cathode, there is an electrolytic reduction of water that results in the formation of hydrogen gas and hydroxyl ions:

$$2\,H_2O + 2\,e \rightarrow H_2\,(g) + 2\,OH^-$$

Metal and hydroxyl ions may combine to form an insoluble hydroxide:

$$M^{n+} + n\,OH^- \rightarrow M\,(OH)_n\,(s)$$

which depends on the metal to be machined and the pH of the solution. The forced flow of the electrolyte removes the precipitated hydroxide and the hydrogen gas together. The heat generated in the gap is removed by the electrolytic flow.

The availability of a suitable tool is one of the most important conditions for successful machining. Generally, this tool should consist of a chemically inert material that is a good electrical conductor. If thin insulating layers are applied at the tool surface, the workpiece can be machined with good dimensional accuracy, resulting in a straight wall. With a non-insulated tool, the workpiece is excessively dissolved opposite the side of the tool, so that a rectangular profile can not be obtained. Copper, steel, molybdenum, and tungsten are suitable metals for the tool.[4,7,8]

Michael Farraday (1791-1867) discovered this general principle of anodic metal removal. It was first used commercially by the Anocut Engineering Company of Chicago in 1959.[7]

There are several advantages of ECM. Costs, such as the capital investment in both the machines and the buildings, are less than for other mechanical machining procedures because of shorter production times and space requirements. Since the metal is dissolved away electrolytically, surfaces are produced consistently that are free from imperfections or work induced stress; hence the

quality of ECM is better than that produced by other methods. Also, there are no burrs or tool wear during machining, so it is possible to produce complicated shapes of large or small area, as well as several components at once.

The main disadvantages of ECM are the difficulties of learning to operate the ECM machine and analyzing the initial costs. Until recently, the selection of tool shape, current density, electrolyte flow rate, and gap width often has been made experimentally because this method was still in the developmental stage.[4,7]

Nowadays, aerospace, automobile and other heavy industries that employ shaping, milling, deburring and finishing operations are applying ECM.[9]

2.2 Electrochemical Micromachining (EMM)

EMM is an application of ECM to microfabricaiton and the process of thin film production. It is regarded as a "greener" method of processing metallic parts in high-tech industries. The EMM method can machine various types of metals and alloys including conductive ceramics and corrosion resistant alloys. The applied current density originated from the Faraday law is the main factor affecting the material removal rate in EMM. In order to obtain a high metal removal rate, proper high electrolyte flow velocities, and high current efficiency for metal dissolution are required.

There are two types of EMM processes for microfabrication: maskless and through-mask. Examples of maskless EMM are: jet EMM- which is localized material removal by the impact of a fine electrolytic jet; and electromilling- which is microfinishing of components and removal of unwanted layers of thin films by

deburring and polishing. Through-mask EMM can be performed using one-sided and two-sided methods. Selective metal dissolution occurs on uncovered areas of a photoresist-patterned workpiece and is accompanied by isotropic undercutting of the photoresist. Production of high-aspect-ratio geometries and minimized undercutting of the photoresist are desirable attributes of the process.[9,10]

In order to achieve proper operation of the ECM process, a high current density (bigger than 100 A/cm^2) is required, but very high concentrations of reaction products may occur, making if possible to only partially remove them by the electrolyte, particularly if the gap between the workpiece and the tool piece is narrow. Increasing concentrations of contaminants can also be deposited on the tool, resulting in non-uniform dissolution of the workpiece. And, changes in the electrolyte composition, elevated temperature, and the electrical resistivity can have an adverse effect on the accuracy. Applying a pulsed voltage, instead of a continuous voltage, can solve these kinds of problems. If the pulse duration and the intervals between the pulses are properly matched to the current density, the contamination within the gap will be completely swept away in between the current intervals.[4,8,9,11]

2.3 Solid-State Welding (SSW)

SSW is the process through which both similar and dissimilar materials are joined together at temperatures lower than the melting point of either of the materials. Diffusion bonding, which is a form of SSW, welds the surfaces together under proper pressure and elevated temperature in a controlled atmosphere.

Deformation joining is the another form, which is achieved by subjecting the surfaces to be joined to extensive deformation. A liquid phase does not form in any of there methods.[12]

2.3.1 Diffusion Welding

Diffusion bonding, solid-state bonding, pressure bonding, isostatic bonding, hot press bonding, forge welding and hot pressure welding can be understood to be synonymous with diffusion welding. By diffusion welding, several kinds of metal combinations can be joined: similar metals can be joined directly, similar metals can be joined with a filler metal between them to provide more complete contact between the surfaces and promote more rapid diffusion, two dissimilar metals can be joined directly, and dissimilar metals can be joined with a third metal, such as a filler metal.

To obtain a satisfactory diffusion weld, two necessary conditions must be met. These are: (a) the mechanical intimacy of faying surface and removal, and (b) the cleaning of interfering surface contaminants to permit metallic bonding. These are important because metal surfaces have several general characteristics such as roughness, chemically reacted and adherent layers, randomly distributed solid or liquid products (oil and dirt), and adsorbed gas or moisture.[13]

2.3.2 Deformation Welding

Cold welding is achieved at near room temperature. The major divisions of cold welding are lap welding, butt welding, slide welding, thermocompression

welding, forge welding, roll welding, extrusion welding, ultrasonic welding, inertia and continuous-drive friction welding, and explosion welding.

- Lap welding is the welding of ductile sheet metal by overlapping the two pieces and applying pressure by means of suitable tools.
- Butt welding is installing wires and rods at the ends of the materials, then pushing them against each other with the proper force to upset the ends.
- Thermocompression welding is a group of techniques to produce deformation welds of ductile face-centered cubic metals at temperatures ranging up to about half of the melting point.
- Forge welding is a hot deformation welding process most commonly applied to the butt welding of steels.
- Roll welding is the stacking of all metal sheets then, passing them through rolls to produce solid-state welds until occurring sufficient deformation has taken place.[12]

2.3.3 Problems in Solid-State Welding

Kirkendall porosity, or vacancy condensation, can occur on the surface of a metal when the diffusion rate of one metal in a couple is much bigger than that of the other metal. Carrying out a postweld heat treatment under hot isostatic gas pressure, or limiting the weld temperature and time will eliminate or minimize this porosity. If welded parts involve thermal cycling, the possible generation of residual stresses owing to the differences of thermal expansion must be considered. If these differences are very large, weld failure can occur even after cooling from

the welding temperature. Also, corrosion can occur after welding pairs, and a brittle weld can result from incorrect use of intermediate foils or interlayers. All variables such as metallurgical, electrochemical, and environmental service conditions must be considered if high-reliability diffusion or deformation welds are required.[12] Finally, intermetallic phases can also form, which can be inherently brittle and reduce the fracture toughness of the joint.

3. DEVICE DESIGN

There are four steps to the creation of a microfloat valve: lamina formation, laminae registration, laminae bonding, and component dissociation. Lamina formation involved two different methods: the first method involved photolithography and laser machining to make a mask and a pattern, then EMM was used to etch the lamina. The second method involved only laser machining. In order to register laminae, a jig was used. After alignment of the laminae, adhesive bonding was carried out at lower pressure and temperature. Component dissociation is a process by which a microfloat valve is made to be a freestanding valve.

3.1. Microfloat Valve Design

As discussed earlier in the Introduction, this research concentrated on the EMM method to make each lamina, while other researchers at OSU have used laser ablation to make lamina. In order to compare with the other researchers' microfloat valves, the design models for each lamina were based on the existing designs.[6]

This microfloat valve consisted of nine laminae (Figure 3). Lamina 1, 3, 5, 7, and 9 were made by the first method, using 76.2 μm stainless steel in the lamina formation. Lamina 2, 4, 6, and 8 were formed by the second method, using 50.8 μm polyimide (Kaptone) in the lamina formation. The first Lamina had an intake air nozzle of with a diameter of 0.9 mm (Figure 3a). Lamina 2, 4, 5, 6, 7, and 8 were of similar design. Lamina 5 and 7 had a hole 3.0 mm in diameter, and

Lamina 2, 4, 6, and 8 had a hole 4.0 mm in diameter so that the lamina's holes would provide the space for a third Lamina to move vertically up and down (Figure 3b). The polyimide laminae's holes were made 1.0 mm wider in diameter than those of the stainless steel laminae, in order to prevent leakage of polyimide during the adhesive bonding step in the laminae bonding process. The third Lamina had the same 3.0 mm diameter hole, but contained a disk of 2.1 mm diameter inside of

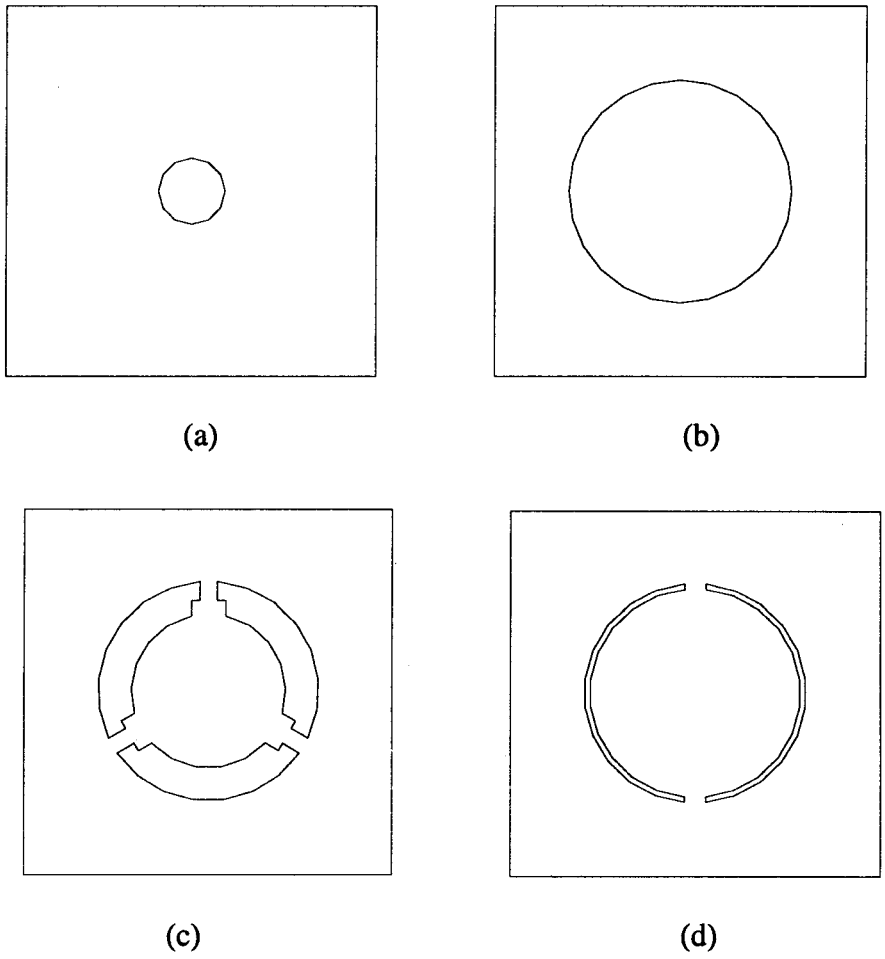

Figure 3. Microfloat Valve Design

the 3.0 mm hole (Figure 3c). The disk was connected to the hole by three small tabs called fixture bridges. The function of the fixture bridge is to keep the disk aligned in the laminae as it moves vertically from the second to the eighth Lamina after dissociation from the three fixture bridges of the third Lamina. The fixture bridges also allow the disk to stand freely. The ninth Lamina is an outtake air nozzle as well as a stop plate for the disk of the second Lamina (Figure 3d). The outside diameter is 3.0 mm and that of the stop plate is 2.85 mm. The stop plate is connected to the other hole by two bridges, each of 0.3 mm width. The design of the fifth Lamina controls the direction of air flow; i.e. air can flow from the first to the ninth Lamina, but not from the ninth to the first.[6]

In order to produce many microfloat valves in a lamina, each lamina was designed to contain 7 microfloat valves. The area of each lamina was 38 mm by 12 mm because the size of the laminae needed to conform with the size of the bonding fixture at PNNL. In order to do EMM, the areas to be etched were made as small as possible to decrease the amount of time required in EMM. In order to make valves of the five stainless steel laminae, the perimeter of each valve was etched to the same width as the edges of the laminae, and the holes were later created by removing the resultant circles. If the etching process were allowed to continue long enough to make the valve hole exactly equal to the desired diameter, then the edges of the laminae would be etched too widely. Etching the perimeter of the hole, and then removing the circle resolved this problem. The lower right edge of each

lamina slopes in order to allow easy identification of each side of the laminae. There are small connection tabs on all laminae to allow electricity to flow across the whole lamina and etch the valves. Specifically, the taps in the laminae were designed to create a conductive connection between the inside and outside of the laminae during EMM. The etched areas are shown in (black) in Figure 4.

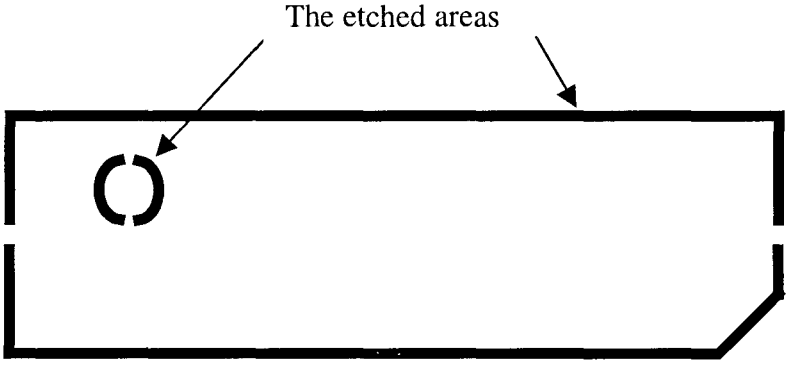

Figure 4. The Design Concept of a Mask

3.2 The Theoretical Orifice Size

The theoretical orifice size was determined in order to compare with former valve designs and to give information to future valve designers. This calculation was drawn from the relationship of compressibility effects in compressible gas flow,

$$Q \equiv CEAY\sqrt{\frac{2\Delta p}{\ell}} \qquad (1)$$

where Q is volumetric flow rate and C is the contraction coefficient.[14] C has a value of one, since the temperature of a device will change little because of the material and size of an orifice. A is the area of the orifice, and E is the velocity of the approach factor, which can be expressed as:

$$E \equiv \frac{1}{\sqrt{1-(A_0 / A_1)^2}} \qquad (2)$$

where A_0 is the downstream orifice area and A_1 is the upstream orifice area. In this instance, A_0 is $\pi * (0.9 \text{ mm})^2 = 2.54 \text{ mm}^2$ and A_1 is $\pi * (6.35 \text{ mm})^2 = 126.68 \text{ mm}^2$ so that the equation for E has a value of 1.

Y is the expansion factor and is expressed by two relationships: $(p_1-p_2)/p_1$ and $\beta = d_0/d_1$ where p_1, is upstream pressure, p_2 is the downstream pressure, d_0 is the orifice diameter, and d_1 is the upstream diameter. Since d_1 = 6.35 mm and d_0 = 0.9 mm, β falls in the range of 0 to 0.2. With the two relationships, Y can be obtained from a chart.[15] The pressure p1 and p2 are determined from test data. The change in pressure is Δp and ρ is the density of gas. With all gathered numbers and data, the theoretical orifice size (d) can be determined using equation (1).

$$d \equiv \sqrt{\frac{4A}{\pi}} \qquad (3)$$

4. METHODS

4.1 Lamina Formation

The laminae for a microfloat valve were created using two different materials, 304 stainless steel 76.2 μm thick, and 50.8 μm polyimide. Laser machining, photolithography and EMM methods were used to create the stainless steel laminae at PNNL. Laser machining was used for the polyimide laminae, made at OSU.

4.1.1. Photolithography

The polyimide (Kaptone, thickness: 127 μm, size: 76.2 mm by 101.6 mm) templates for Lamina 1, 3, 5, 7 and 9 were mounted to glass slides using rubber cement, then rolled with a roller to make the polyimide adhere to the glass slide. The CIM-CAD program was converted to a laser machine language and the polyimide templates were exposed to the laser 3 times for 18 hours to make a mask (Figure 5). The laser micromachining system used was the Potomac LMT-5000, which has a TGX-1000 248-nm Excimer laser, an aperture of approximately 10 μm, and a depth of about 127 μm. Lamina 1, 5, 7, and 9 were created on one polyimide template, and Lamina 3 was created separately on a second polyimide template, due to the different etching times required in EMM. After laser machining, the excess polyimide was removed. The polyimide etched during EMM processing remained stuck to the glass slide. Residual rubber cement left on

the machined polyimide was used to mount the machined polyimide to new slides. The masks generated by these steps were used in photolithography.

Next, the substrates were prepared. Pieces of stainless steel 76.2 μm thick were cut to a size of 76.2 mm by 101.6 mm for Lamina 1, 5, 7, and 9, and 50.8 mm by 76.2 mm for Lamina 3. These were degreased in a hot vapor degreaser (1.1.1 Trichloroethane) for 10 minutes. The substrates were washed with a micro soap solution (available from International Products Corporation), the liquid laboratory cleaner for critical cleaning. 2.5 ounces of solution were mixed with one gallon of warm water, then rinsed with deionized (DI) water, and dried with nitrogen.

Before starting photolithography with the substrates, the oven was set to 90°C, and the vacuum pump was started. The stainless steel pieces were mounted to glass slides with scotch tape to keep the steel flat. The spin speed was calibrated to 3000 rpm. Photoresist was poured onto the backside of the substrate and the substrate was spun at 3000 rpm for 20 seconds. AZ 4903 photoresist generally provides spin-on film thickness of 7-30 μm and is used for thick resist. About 4.5 μm spin-on film thickness were provided here. After a 20 second spin cycle, the stainless steel substrates were baked at 90°C for 30 minutes. The duration and temperature of baking must be precise, as any deviation from these conditions will alter the effect of Ultra Violet (UV) exposure after the substrates are baked. Specifically, when baked at temperatures over 90°C, the bonds of the materials become so strong that they can not be released during UV exposure. The tape was peeled off of the glass slides, and the front (other) side of the stainless steel

substrate was mounted to fresh glass slides. The photoresist, spinning, and baking procedure was then repeated at the same conditions.

The stainless steel substrates and the laser machined masks were set on the UV machine on "I" line exposure station (365nm UV). The mask was placed on the upper side, and the substrate on the lower side. It was very important to maintain a strict parallelism between the mask and the substrate; otherwise, a shadowed area was generated during UV exposure. The stainless steel substrates were exposed to UV for 360 seconds at 17.5 mW/cm^2.

Finally, the substrates were developed in 421 developer (four parts developer to one part DI water) with 1000 cc Pyrex glassware for rinse and developing beakers. The substrate was dropped into the developer and agitated for 75 seconds (standard develop time). If the substrates are developed for longer than 75 seconds, the edge areas will not be straight. After developing, the substrate was rinsed in DI water for 60 seconds and dried with nitrogen. The substrate was then inspected by microscope.

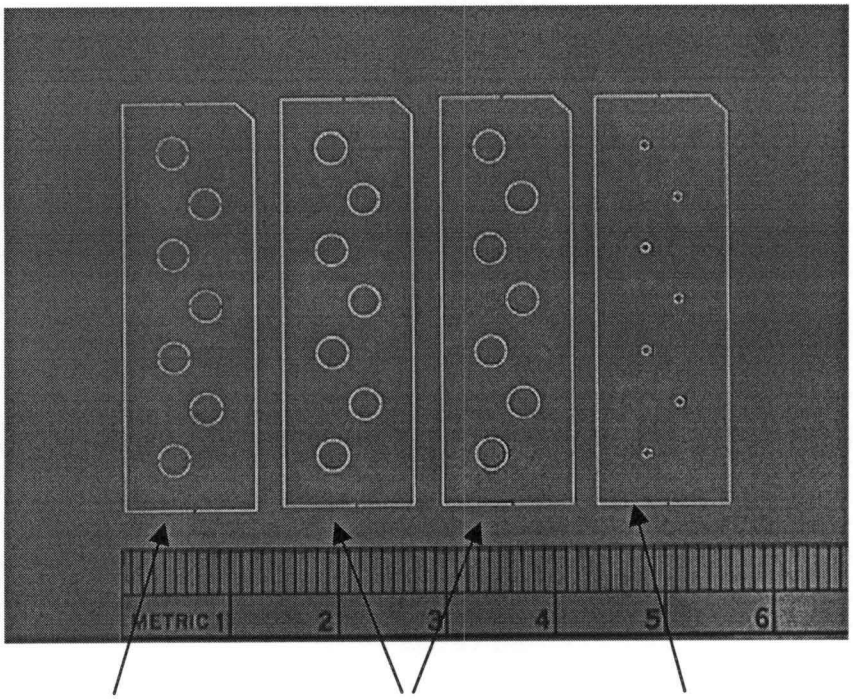

Lamina 9 Lamina 5 & 7 Lamina 1

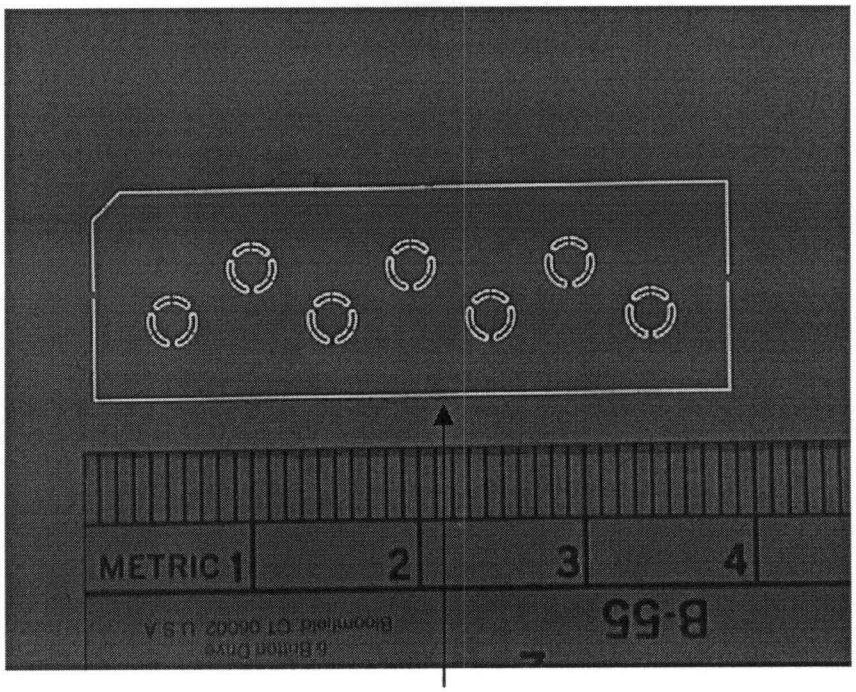

Lamina 3

Figure 5. Masks Created after Laser Ablation

4.1.2. EMM Process

Before starting with the EMM machine, two support items had to be created. A pulsed DC power supply that produces a pulsated voltage instead of a continuous voltage was built by a technician at PNNL. The pulsed voltage uses pulses of 1 ms duration with an interval of 10 ms between them. In addition, a fixture that holds the workpiece and the tool was built.

There are two different methods of using tools, which are known as soft tool and hard tool methods by OSU researchers. A soft tool uses a lithography mask so that the etched area is not covered by photoresist. For the soft tool method, a pulsed DC power supply and a feeder mechanism (a positioning mechanism) are needed. A feeder mechanism moves toward the workpiece during EMM because the gap between the tool and workpiece should be maintained. Generally, the EMM procedure uses this soft tool method. The hard tool method uses a master tool that has the same geometry as the etched area, but with smaller dimensions. This master tool is usually fabricated by mold micromachining. Due to time and budget constraints at PNNL, a soft tool method was selected for this thesis. Also, a feeder mechanism could not be prepared, so a fixture was built instead.

The stainless steel work piece with the photoresist etched pattern was mounted to the lower side of the fixture. Then, a 76.2 μm thick nickel tool of the same size as the workpiece was mounted on the upper side of the fixture

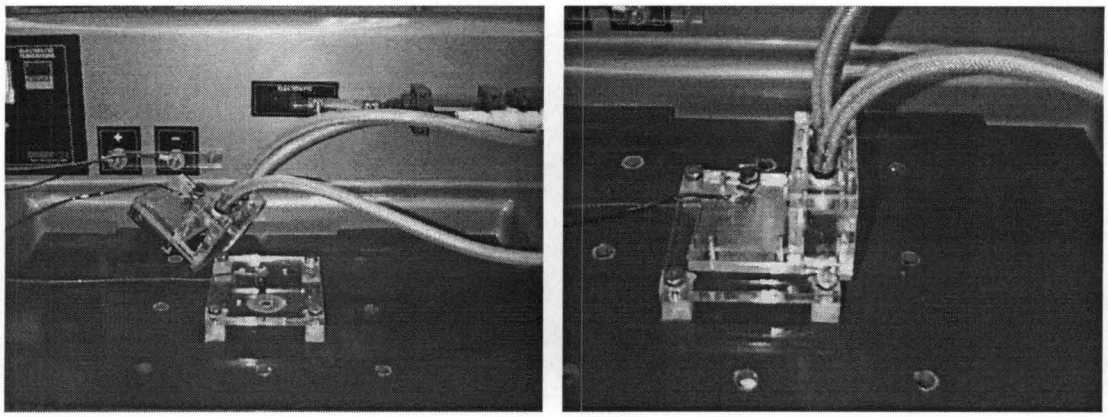

Figure 6. Fixture for EMM

mechanism. The fixture was assembled to set a gap between the workpiece and the tool of 2 mm. After the temperature of the electrolyte solution (pH 6.95) was stabilized at 62°C, the electrolyte was allowed to fill up the inside of the fixture through three hoses, taking care to prevent the formation of bubbles (which can disrupt the EMM). The voltage of the EMM was increased to approximately 20 V in order to attain a current of 100 A, which was the maximum current the pulsed DC power supply could produce. According to a former study[4], 2 to 40 V is a proper operating voltage for a narrow gap (20 to 200 μm) with a current density ranging from 10 to 1000 A/cm^2.

The etch time was around 2 minutes for the stainless steel substrates that formed Lamina 1, 5, 7, and 9. Lamina 3 required a longer etching time of 2.5 minutes since it had more area to be etched. When EMM was initially formed, all five of these laminae were designed at the same substrate, and it was discovered

that Lamina 3 required a longer etching time than the others. If all laminae were etched for the same length of time as Lamina 3, then they were etched beyond the required areas.

During EMM, it was found that the areas to be etched were not etched at the same rate. The 38 mm by 12 mm rectangular perimeters were etched in the first minute, followed by the perimeters of the interior circles, until all areas were fully etched by 2 minutes. In Lamina 3, whose valves had inside and outside perimeters to be etched in order to create the fixture bridges (Figure 7).

After EMM, the fixture was disassembled, the tape peeled off, and the etched substrate removed; this substrate were cleaned with DI water and with acetone, and degreased in the hot vapor degreaser.

After EMM, all laminae were examined under microscope to verify their dimensions. The diameters of most of the holes in the laminae were bigger than 50-100 μm. Also, the geometries in the backsides of laminae were a little bigger than in the front sides, which means over etching and under cut had occurred. Future studies should produce the exact dimensions. For instance, the etch time should be shorter and the dimensions of all masks should be smaller sizes than the sizes that are produced after EMM. In addition, a feeder mechanism should be used in order to prevent under cut; particularly for, thicker materials.

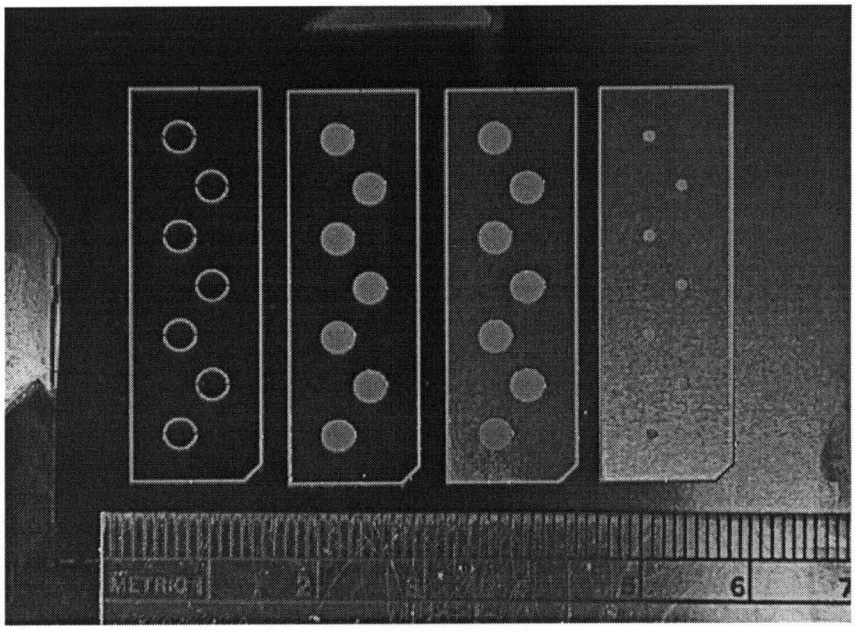

Lamina 1, 5, 7, and 9

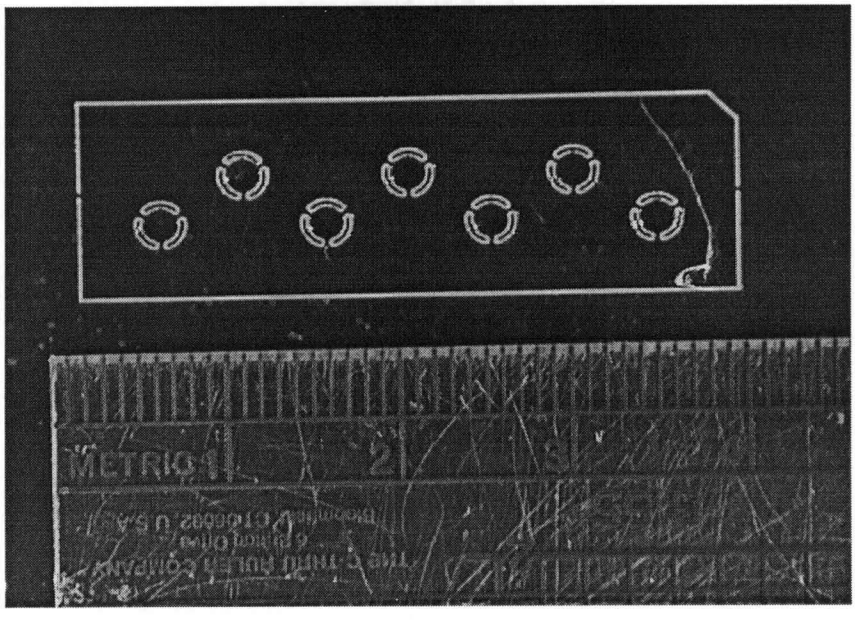

Lamina 3

Figure 7. Laminae Created after EMM

4.1.3 Laser Micromachining

At OSU, Lamina 2, 4, 6, and 8 were created with 76.2 μm polyimide (Kaptone) with a design similar to that of Lamina 5 and 7, but with two different sizes. The diameter of the polyimide Lamina was 4 mm because melt material could clog the inside of the holes in the stainless steel laminae and reduce valve performance. Since the actual size of the stainless steel laminae was smaller than 38 mm by 12 mm, the size of the polyimide laminae was set at 37 mm by 11 mm after measuring all sizes of the stainless steel laminae.

The laminae were designed using the AutoCAD program and then converted to SmartCAM by DXF files. Using SmartCAM, the converted files were set up for the ESI 4420 laser machine. The files were translated to LIF files with the LIFUTIL program in the computer. Then, the translated files were transferred to the computer of the ESI 4420 laser machine, which machined each lamina. After machining, each lamina was cleaned with methanol, acetone, methanol again, and DI water. Finally, the lamina was blown dry with air.

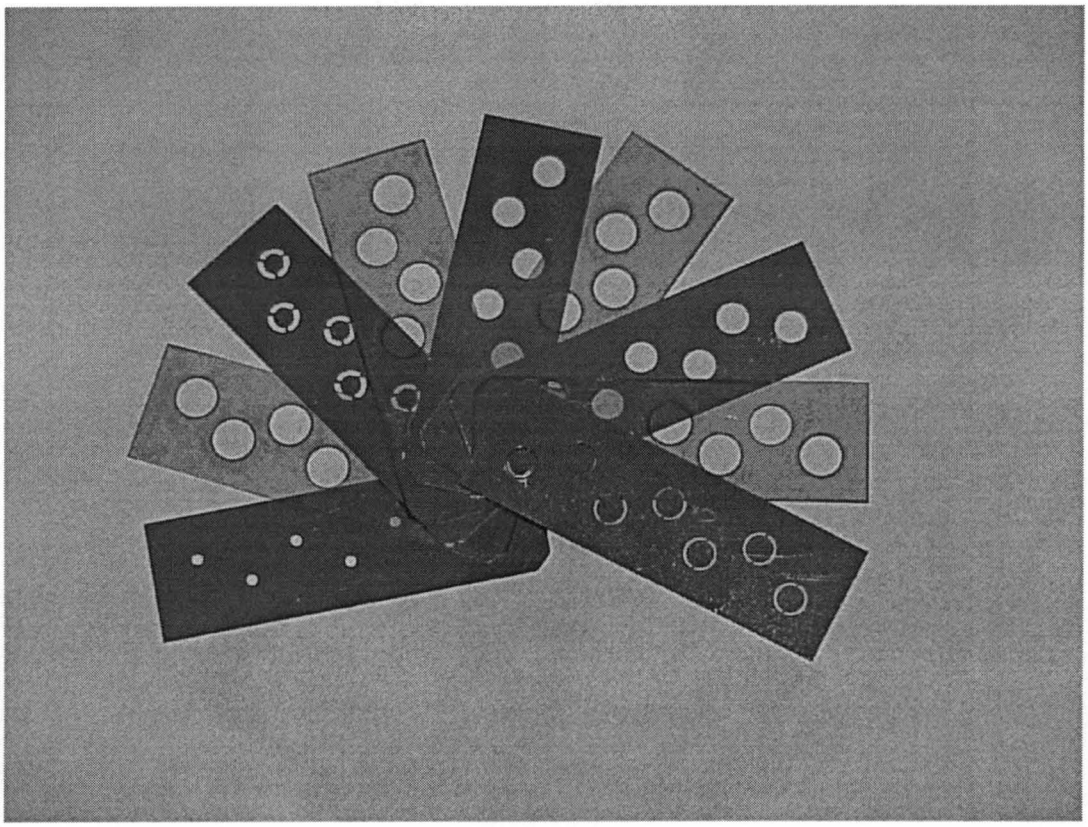

Figure 8. Finished Laminae

4.2 Laminae Registration & Bonding

Laminae registration is the most important step among the four for making a microfloat valve. If the laminae registration is not precise, the microfloat valve can not perform all of its functions. Also, all laminae should be bonded with the optimized bonding values. Two different bonding methods, diffusion bonding and thermal adhesive bonding, were tried.

4.2.1 Diffusion Bonding

At PNNL, a special jig was designed to register metallic shims such as copper, aluminum, and stainless steel for diffusion bonding (welding) using high temperature and pressure.[15] The principle of jig for the registration of laminae was edge alignment. The laminae are aligned with each other with respect to two of the edges of each lamina. In order to do diffusion bonding at PNNL, only stainless steel laminae were used because polyimide laminae would not permit bonding at high temperatures. A vacuum hot press was used at 600°C and 41,370 kPa (6000 psi) for 2 hours for this bonding.[15]

4.2.2 Thermal Adhesive Bonding

A similar jig existed to register laminae such as copper, steel and polyimide at OSU using thermal adhesive bonding at lower temperature and pressure. The principle of both jigs in the registration of the laminae is the same as in diffusion bonding (See Figure 9).

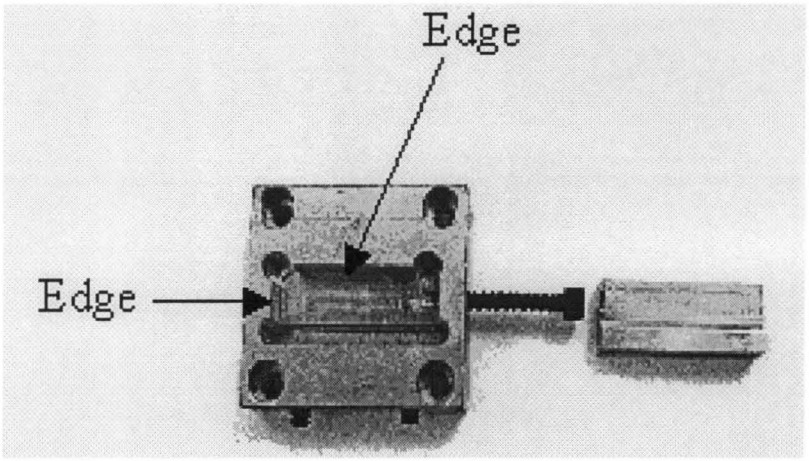

Figure 9. Jig for Laminae Registration in Thermal Adhesive Bonding

Polyimide has good physical, electrical and mechanical properties over a wide temperature range, and is especially useful in applications involving high operating temperatures. Polyimide has adhesive properties, so it can bond surfaces together when heated and compressed.

Adhesive bonding needs only a powerstat, a resistance heater, a thermal couple (electric sensor), and a torque wrench to apply pressure. Adhesive bonding conditions are much less extreme than those for diffusion bonding, being 260°C at 1380 kPa (200 psi) for 10 minutes. Polyimide laminae were designed to be the same size as the stainless steel laminae and were inserted between pairs of stainless steel laminae to act as an adhesive for the stainless steel laminae.

The optimal values for bonding the laminae were determined using the STAT Graphics Plus 3.0 program. The design class was Response Surface and the number of responses was defined as bonding condition. The allowed number of

experimental factors in the program is two, so time and temperature were chosen as the manipulated variables. An additional factor in this experiment, pressure, could not be included as a condition in this program, so it was fixed at 135 kPa. The experimental ranges for temperature and time are shown (below) in Table 1.

Table 1. Factors for Experimental Design

Factors	Low	High	Units	Continuous
Temperature	230	270	°C	Yes
Time	0	15	min	Yes

In order to determine the optimal value for bonding, the bonding conditions were scored from zero for no bond formation at all, to nine for a complete seal with no flash (Table 2), and then the program suggested 10 randomized runs (Table 3). These predictive values were used to set the bonding condition based on the scores assigned to the different hypothetical conditions. In Table 1, the highest and the lowest temperatures are 230°C and 270°C. These values were determined based upon experiments. If the laminae were bonded at a temperature over 270°C, the holes in the steel laminae would be completely blocked by polyimide. If the laminae were bonded at a temperature below 230°C, they would not bond at all. Similar results were predicted for the longest and shortest bonding times. The times shown represent waiting time after reaching the desired temperature. In order to evaluate the hypothetical bonding conditions, an evaluation standard was devised

Table 2. The Evaluation Standard for Bonding

Score	Case	Definition
0	H	Flash blocking all inside of the laminate 9
	L	No bond at all
1	H	Over 80% block of the laminate 9
	L	Peeled off easily
2	H	50-80% block
	L	More than 50% of bubble beneath the Kaptone
3	H	41-50% flash
	L	41-50% bubble
4	H	31-40% flash
	L	31-40% bubble
5	H	21-30% flash
	L	21-30% bubble
6	H	11-20% flash
	L	11-20% bubble
7	H	6-10% flash
	L	6-10% bubble
8	H	1-5% flash
	L	1-5% bubble
9		Completely sealed together, no flash

Note: H= Too high temperature or longer time
L= Too low temperature or shorter time

Table 3. Randomized 10 Runs

Run	Temperature (C)	Time (min)	Bonding Condition
1	270	0	2
2	230	0	7
3	250	7.5	8
4	230	15	7
5	250	0	7
6	271.5	7.5	4
7	228.4	7.5	4
8	270	15	5
9	250	15.58	7
10	250	7.5	8

(Table 2).

After cleaning, all laminae were aligned in a jig. When the laminae were aligned, Lamina 3 and 7 were turned over so that the backs were aligned as front sides. After EMM, the etched areas in the backs of the laminae were bigger than those in the front sides, so flipping those laminae yield a smoother sidewall inside of the microfloat valve.

After putting all laminae into the jig, the cover was closed and one edge was aligned by tightening one bolt while the other was tightened by two bolts. The jig was put into the middle of two equally sized pieces of bronze, which allowed heat coming from the Powerstat to be applied, resulting in increased bonding temperature. All three pieces were then held together in a fixture, and pressure was applied to the laminate by a PROTO dial torque wrench. The Keithley 740 system scanning thermometer was connected to the jig to measure temperature. Finally, 135 kPa of pressure was applied to the jig with the dial torque wrench and the powerstat set to 135. Once the temperature reached 248°C, the powerstat was shut off and the assembly left standing for 13.5 minutes. Although the hypothetical design analysis indicated an ideal waiting time of 14.5 minutes, experimental trial and error revealed that 13.5 minutes was the preferred waiting time.

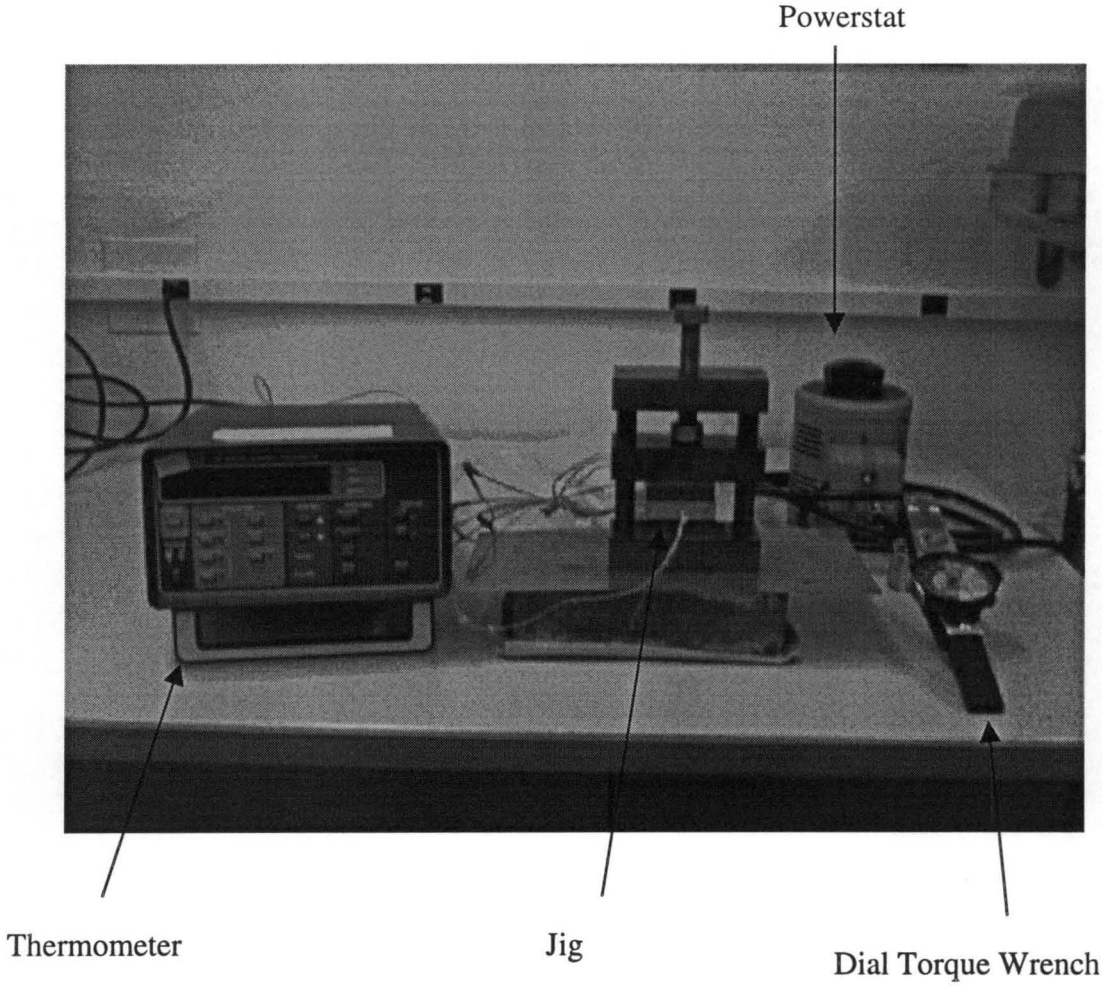

Figure 10. Laminae Bonding

4.3 Component Dissociation

In order to make a complete microfloat valve, the third Lamina, which has three fixture bridges, needed to be dissociated to become a freestanding valve. This method is called Component Dissociation and was created at OSU.[6] However, an improved method is required to dissociate an electrochemical micromachined valve

here. The thickness of the stainless steel lamina is 76.2 μm, which is one half the thickness of the lamina previously produced in research at OSU. Furthermore, the dimensions of the valve are smaller than those of the former valve. A fixture and a capacitor bank to dissociate it used the same facilities as the older valves, but an anode probe, which is anchored to the fixture, and a cathode bar, were built. The anode probe is controlled by a manual dial, which permits slow and precise movement so as to prevent exerting high pressure on the disk of Lamina 3 (Figure 11).

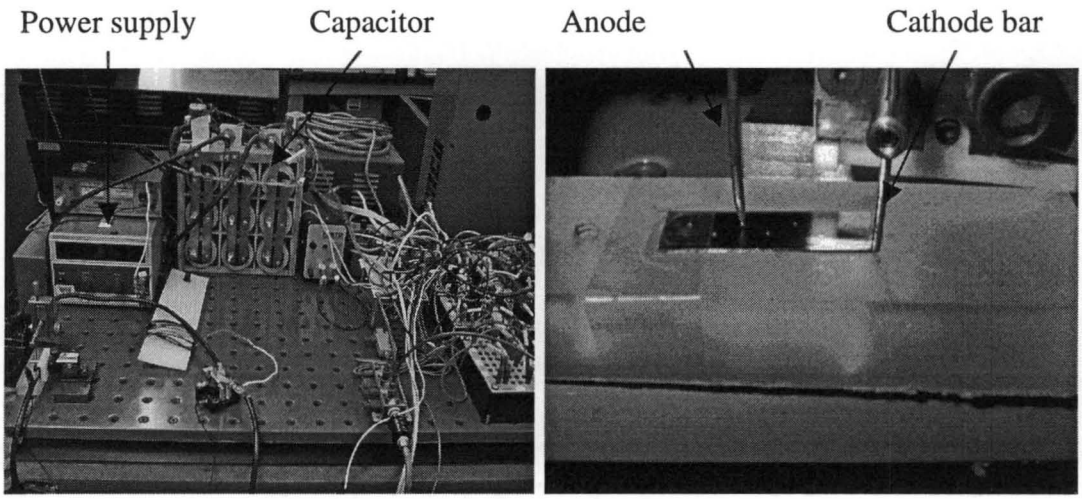

Figure 11. Component Dissociation

This means that the anode probe is inserted through the 0.9 mm hole of the first Lamina until it touches the disk of Lamina 3. The cathode bar is connected subsequently to the slope-edge side of the valve by using a manual dial. A power supply charges the capacitor, then the capacitor discharges across the device. Finally, the fixture bridges of Lamina 3 are dissociated (vaporized) and the disk is freestanding and able to move.[6]

The proper voltage and current were determined after experimentation by using sample microfloat valves cut by laser machine, instead of EMM. There were 9 capacitors, each rate at 10,000 μF. The optimized voltage was different at different current, such as 5 V at 70,000 μF and 4.25 V at 90,000 μF. For this study, 4.25 V at 90,000 μF was set as the optimized value, but a higher voltage, 7 V, was needed to dissociate the three fixture bridges for the EMM microfloat valves, since the fixture bridges produced by EMM were bigger and wider than those produced by laser machining.

4.4 Valve Performance Test

After dissociation, each valve was tested for pressure drop and the valves were evaluated by diodicity. The pressure drop test loop was recently created at OSU so that most meso- and micro-sized devices can be tested using either fluids or gases. However, the test loop was simplified to allow comparison with the microfloat valve that was created by laser ablation in a former study.[6] The test loop used a compressed air inlet, two 5-way valves, two ball valves, a flowmeter, a

pressure gauge, a pressure transducer and a device (laminate) (Figure 12). Each valve in a laminate was tested separately to determine its diodicity. A fixture was built for the test loops that could be clamped with a lever, sealing the valve with two gaskets. In order to discover whether or not a valve was leaky, soapy water was applied to the surrounding areas of the fixture, including the gaskets and valves and observed for the formation of bubbles when pressurized.

The outlet air flow was allowed to flow freely, so the outlet pressure was assumed to be at standard atmospheric pressure (1 atm = 101,325 Pa). This meant that the outlet flow and low pressure lines were not connected through the test loop. The pressure on the pressure gauge was read as the inlet pressure and the transducer was used in calibration. The maximum pressure of the transducer was 172 kPa (25 psi) while the maximum tested pressure was 448 kPa (65 psi). Within 172 kPa, the difference between the pressure gauge and transducer was lower than 1%.

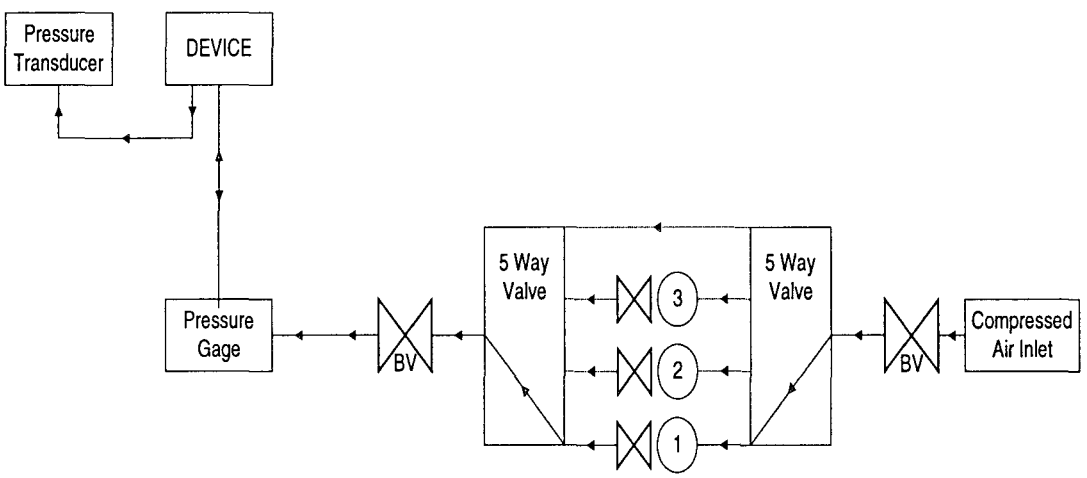

Figure 12. Schematic Diagram of the Test Loop

5. RESULTS

5.1 Diffusion-bonded Valve

As mentioned in Chapter 4, diffusion bonding was attempted with using only stainless steel laminae at PNNL. A microfloat valve consisted of total 5 laminae. The lamina, which had fixture bridges, was Lamina 3 and the laminae, which had 3 mm diameter holes, were Lamina 2 and 4.

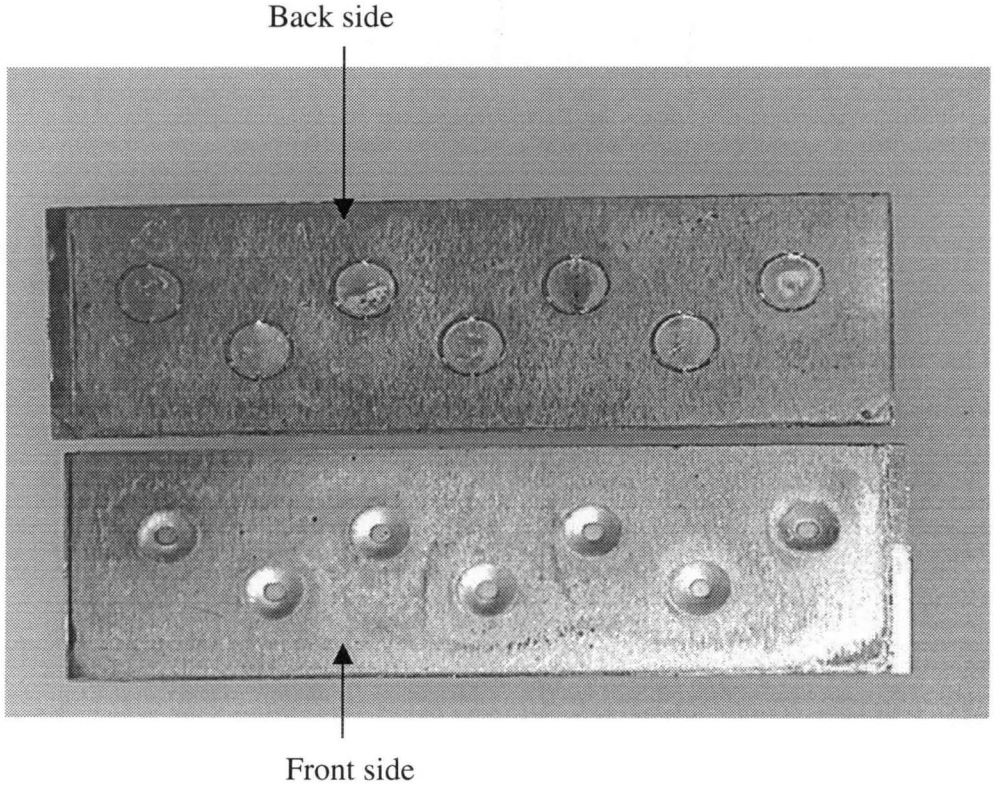

Figure 13. Diffusion-bonded Microfloat Valves

After bonding, Lamina 1 was forced into lamina 2 due to thermal expansion effects (See Figure 13). At OSU, component dissociation has been carried out with diffusion-bonded microfloat valves, but the process failed to dissociate fixture bridges. Since the gap between Lamina 3 and Lamina 5 was very small, the stop plate of Lamina 5 was dissociated together with the fixture bridges of Lamina 3. In order to create a microfloat valve, the gap should be increased and adhesive bonding method was needed.

5.2 Adhesive-bonded Valve

For the adhesive bonding method, all stainless steel and polyimide laminae were used. After component dissociation, the pressure drop test was carried out and the theoretical orifice size calculated in order to measure each valve's performance.

5.2.1 Process Parameter Selection

After evaluating the 10 runs against the evaluation standard, an "Analysis Design" program was run to predict the best bonding conditions (Figure 14). In the Figure 14, the smallest contour that is located in the center and top of the graph is the optimized value to bond laminae. For example, at 248°C the waiting time is 14.5 minutes.

After taking out the bonded microfloat valve, the registration of the laminae and any flash leaked into the valve were inspected by comparing the edges of

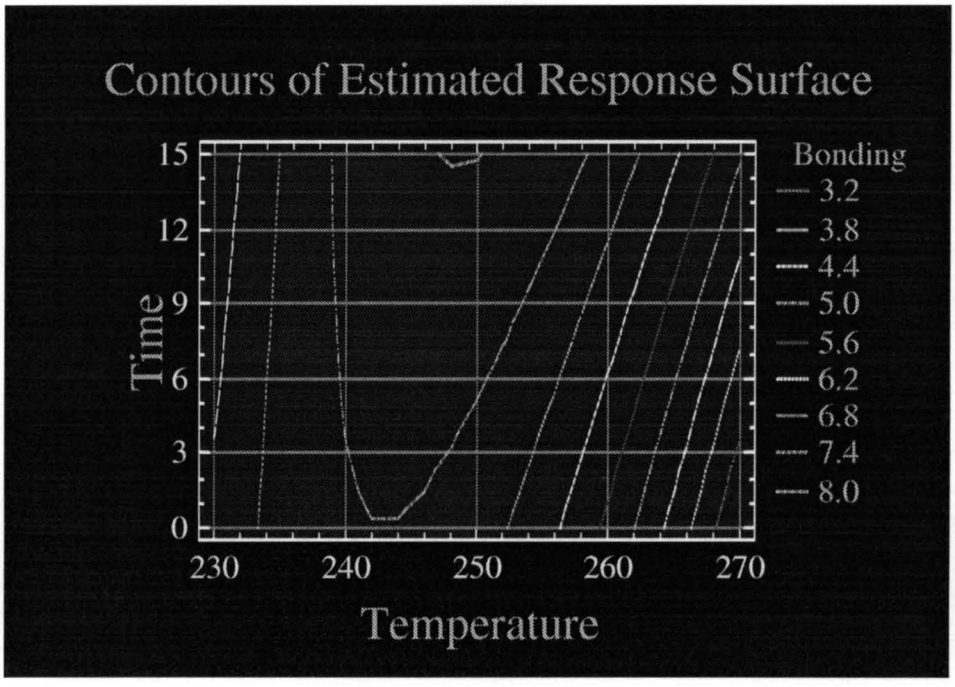

Figure 14. Contours of Estimated Response Surface

Lamina 9 with each 38mm by 12mm edge. Although the valves showed no evidence of flash, the laminae were somewhat misregistered, especially Lamina 9 and 3. Misregistration may be the result of one or more experimental errors. First, the laminae were not etched perfectly enough to match precisely (Lamina 9 and 3 were different sizes). Second, the jig used here may have been a limiting factor because three bolts, rather than two, adjusted registration. If only two adjustments had been used for the registration, the additional source of variation would have been avoided. Third, the different sizes of the stainless steel and polyimide

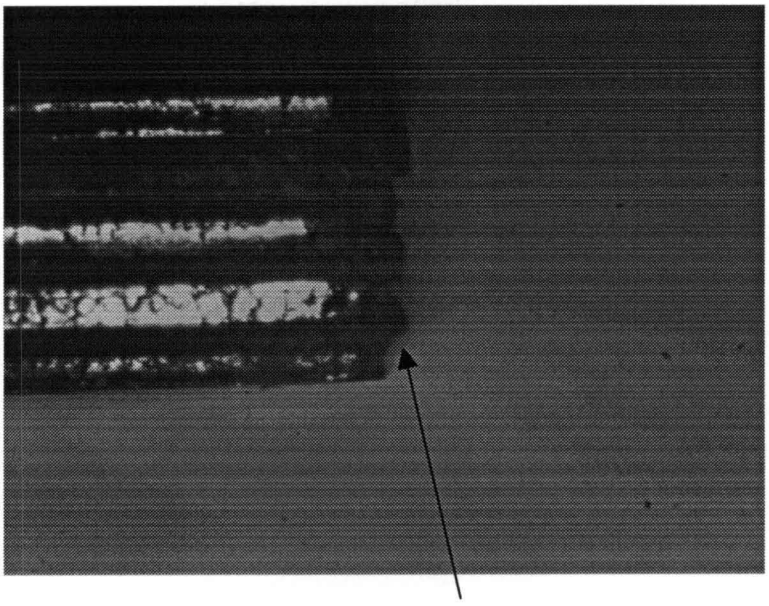

The Edge of A Valve

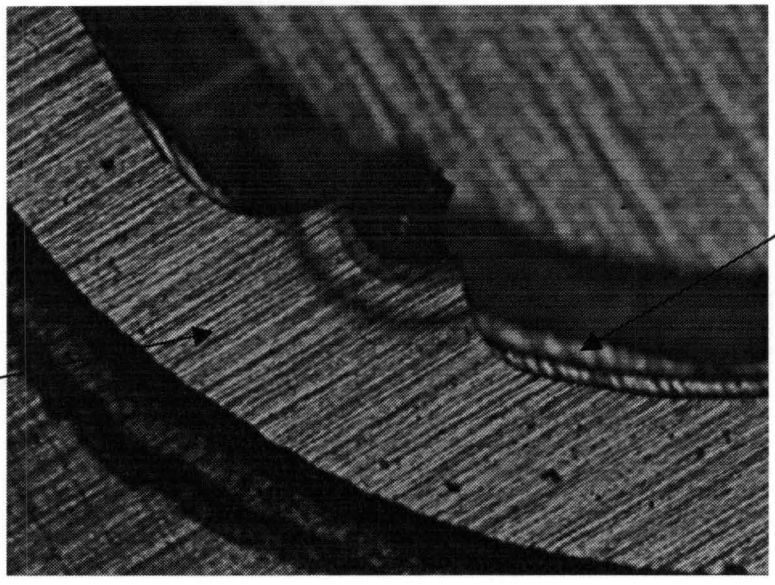

Figure 15. Bonded Laminae

laminates might have adversely affected registration. Finally, the jig, which was made of bronze, might have caused misregistration due to long term wear.

5.2.2 Valve Performance

Diodicity is defined as flow rate divided by leakage rate at a constant pressure. Thus, higher diodicity is indicative of better performance. A total of 16 microfloat valves were tested to identify the valve having the highest average diodicity over a range of pressures. Then, the maximum and mean diodicities of only the best valve were compared to the best values determined in the previous study.[6]

Table 4. Calculated Diodicity for the Best Valve

Pressure (kPa)	Flow rate (ml/min)	Leakage rate (ml/min)	Diodicity
34.5	173	28	6.18
103.4	269	28	9.61
172.4	337	30	11.23
241.3	390	30	13.00
310.3	443	30	14.77
379.2	486	31	15.68
448.2	518	31	16.71
			12.45 (Average)

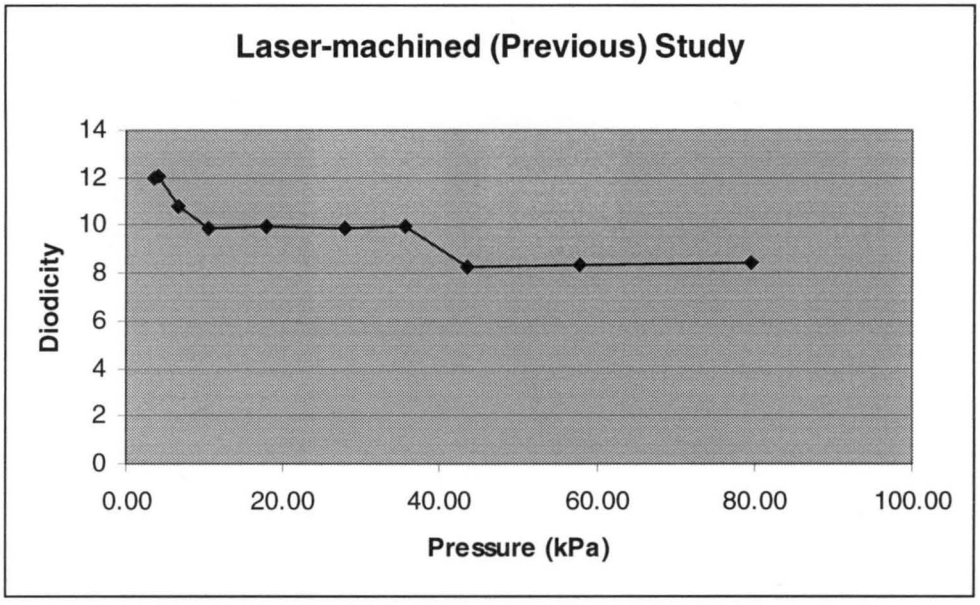

(a)

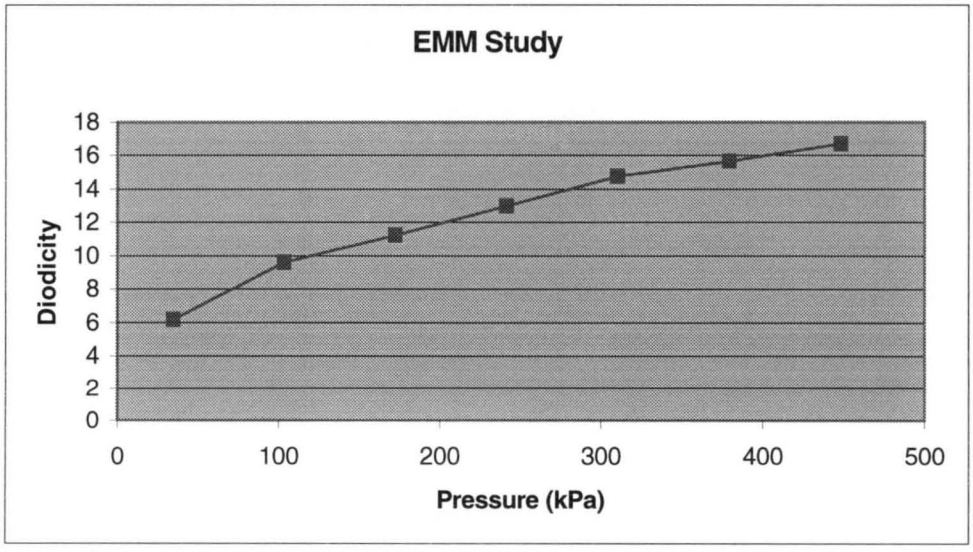

(b)

Figure 16. Laser-machined Vs EMM Diodicity

The average diodicity for the best valve in this study was 12.45, with the maximum value of 16.71 being reached at 448 kPa. The best average and maximum values from the previous study were 11.19 and 17.10, respectively. The previous study (See Figure 16a), the diodicity peaked at approximately 4 kPa and steadily decreased until the testing ceased at 80 kPa. However, in this study (See Figure 16b), the maximum diodicity was reached at 448 kPa after steadily increasing over the entire test range. Testing ceased at this point due to flow loop testing limitations being exceeded. The trend indicated that further increases in pressure would results in improved diodicity, contrary to the results of the previous fabrication method. Statistical evaluation of the typical results was not possible because only the best obtained valve was reported in the previous study.

Since the two valves used different fixtures and test loops, comparison of the two based upon the reported data was not very precise. If both studies had used the same test loops, the comparison between the results might have been more informative and valid.

5.2.3 Results for Theoretical Orifice Size

For maximum efficiency, the calculated (theoretical) orifice size is equal to the actual (measured) orifice size. Using the equations in Chapter 3, the theoretical orifice size for each valve was calculated. This result is also a good predictor of the performance of a microfloat valve, as well as useful data for future valve designers. Table 5 shows the calculated values at the observed flow rates and Figure 17 shows a graph of theoretical orifice sizes at different pressures for the valve fabricated in this study. The average theoretical size predicted by the equations in Chapter 3 was 0.24 mm, whereas the experimental orifice size was 0.9 mm. The ratio of calculated size to actual size for this study was 26%. However, the values in the former study, which were 0.629 mm for the theoretical orifice size and 1.5 mm for the actual orifice size, yield an improved ratio of ratio of 42%. This indicates that the fabricated valve from first study was more efficient than the current processing method.

Table 5. Calculation of the Theoretical Orifice Size

R (Air) = 287 m^2/(K*s^2) 1 atm = 101325 Pa
Temperature = 298.65 K

Flow rate (Q) (cm^3/sec)	Expanssion Factor (Y)	Delta P (kPa)	(p1-p2)/p1	Density (kg/m^3)	Orifice Area (cm^2)	Orifice Size (mm)
2.88	0.750	34.5	0.25	0.4	0.00009	0.17
4.48	0.760	103.4	0.51	1.21	0.00014	0.21
5.62	0.770	172.4	0.63	2.01	0.00018	0.24
6.50	0.785	241.3	0.7	2.82	0.00020	0.25
7.38	0.815	310.3	0.75	3.62	0.00022	0.26
8.10	0.848	379.2	0.79	4.42	0.00023	0.27
8.63	0.930	448.2	0.82	5.23	0.00022	0.27
						0.24 (Average)

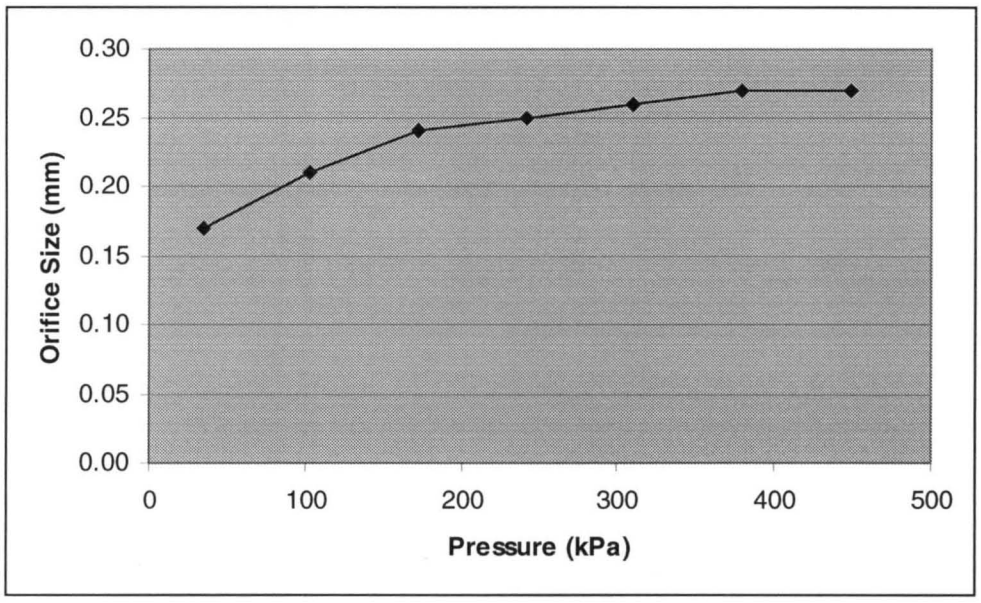

Figure 17. Theoretical Orifice Size

5.3 Discussion

After dissociation, the valves were peeled off with a sharp knife to investigate the three vaporized areas by microscope. In Figure 18, the end view of float shows "black ball" produced by dissociating the fixture bridge: A) float thickness = 76.2 μm, and B) "black ball" thickness = 138.5 μm. All vaporized areas had this black colored ball that was two times thicker than the thickness of the stainless steel laminate, which indicates that the disk could not completely cover Lamina 1 to prevent the flow of fluid from Lamina 9 to Lamina 1.

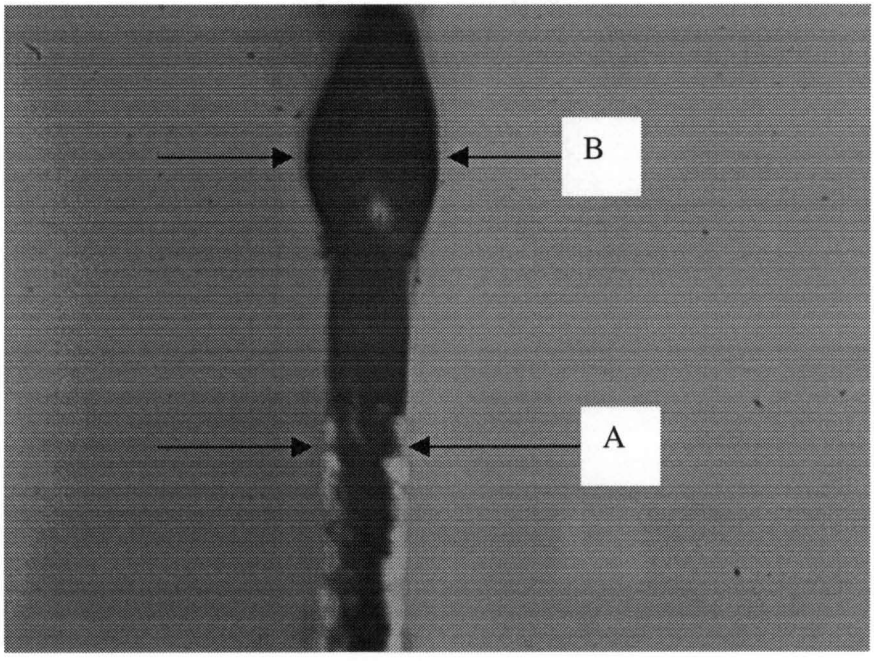

Figure 18. End view of float showing A) the original thickness of the float = 76.2 μm and B) the thickness of the "black ball" after component dissociation of the fixture bridge = 138.5 μm.

After the performance test, air was supplied with an air nozzle to check whether the disk of Lamina 3 moved well or not. While air was delivered to the backside (Lamina 9), the disk moved up and down freely, but a small gap between the orifice of Lamina 1 and the disk of Lamina 3 was found and some air leakage was discovered by finger touch at the orifice of Lamina 1. After EMM, the size of the orifice was bigger than 0.9 mm – the actual size was close to 1.0 mm, but the size of the disk was smaller than 2.1 mm – the actual size was less than 2.0 mm.

Furthermore, the three fixture bridges of the disk were dissociated at points very close to the disk area, which interfered with maintaining the disk in the center of the orifice. Specifically, the smaller surface area of the disk (resulting from the dissociation of the fixture bridges at points closer to the disk than called for by the design) allowed the formation of a gap. This gap decreased diodicity. Moreover, the disk did not completely cover the orifice, because the end of each fixture bridge had a big black ball that was two times thicker than the thickness of stainless steel. This is another factor that may have contributed to a lower diodicity estimate.

In Figure 16b, the diodicity was increased as the pressure was increased. This result is to be expected since the disk could bend more and close off a greater amount of the area of the orifice when high pressure was used in the leakage test, while at lower pressures, there were lower bending forces to aid in closing the orifice.

In future studies, all of these listed problems should be reconsidered in the design of a new microfloat valve. The fixture bridges areas should be shorter and narrower to be vaporized easily. The tap areas should be bigger, so that fixture bridge and tap can be clearly distinguished after EMM. And, all interior dimensions should be made smaller than the dimensions desired to counteract overetching during EMM (See Figure 19).

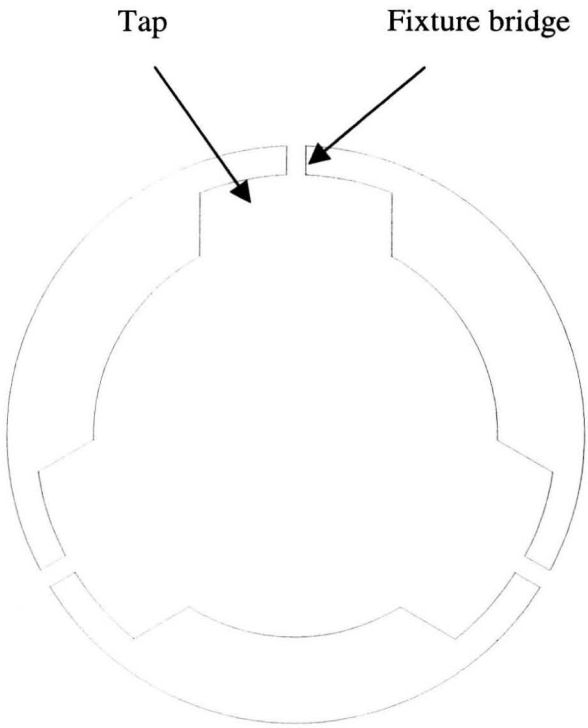

Figure 19. New Microfloat Valve Design

6. CONCLUSIONS

6.1 Summary

The primary contribution of this study is the creation of a valve that has a higher potential diodicity ratio. A further contribution is that this study demonstrated that EMM does not redeposit material around machined areas after machining, unlike laser ablation. A ridge of redeposited material decreases diodicity.

Four steps were carried out to create the microfloat valve: lamina formation, laminae registration, laminae bonding and component dissociation. A total of nine laminae made up the microfloat valve. Lamina 1 was an orifice to permit inlet flow, and Lamina 3 was comprised of a disk having three fixture bridges that could freely stand after dissociation. Lamina 9 functioned as a stop valve, and the remaining laminae formed the inside cylinder of the valve.

304 stainless steel of 76.2 μm thickness was used for Lamina 1, 3, 5, 7and 9, and 50.8 μm polyimide was used for the other laminae. Photolithography and EMM methods were used to create the stainless steel Lamina 1, 3, 5, 7 and 9, and laser ablation was used for polyimide Lamina 2, 4, 6 and 8.

In the EMM method, the laminae created were smaller in size than the designed size since overetching had occurred. However, the machined areas did not have redeposited material, and some areas had straight walls.

In the laminae registration step, Lamina 3 and 9 did not have expected dimensions, which resulted in slight misregistration. In addition, the fixture for bonding was not perfectly aligned. In the component dissociation step, the dissociated areas were bigger than the thickness of stainless steel. At the performance test, the average diodicity of the best microfloat valve was 12.45 and with a maximum of 16.71 obtained at 448 kPa.

Overall, this study showed that EMM can potentially produce better cleaned and machined surfaces that do not have redeposited materials, in contrast to laser ablation, which results in surfaces with substantial amounts of redeposited materials (See Appendix B). The diodicity attained in this study indicates an improvement over that in former studies, and identifies some means for the potential of EMM to generate much higher diodicities in the future. In addition, as discussed in the Introduction, this study shows that high volume, low-cost production could be achieved by using microlamination methods. Further, higher aspect-ratio (high-to-width) structures can be realized by using the EMM method in the future.

6.2 Recommendations for Future Study

In the EMM method, effort should be made to generate materials with better machined surfaces. First, the predictions of the theoretical EMM equations could be followed with respect to current and voltage at the machining areas, as well as a flow rate and velocity of the electrolyte to make better microfloat valves. Second, a feeder mechanism should be used to produce a straight wall. Such a mechanism

would prevent overetching, so that a straight wall could be produced in thick (more than 254 μm) materials. Last, the design of the interior mask features should be smaller than the actual size to prevent over etching.

For laminae registration, a highly precise fixture should be built and registration methods should be studied further. Rather than using three bolts to register laminae, a two-edge registration method could be adopted. This method would result in better alignment due to lower variability potential. In order to get better bonding, a hot-press machine can be used to bond laminae. This machine would be more reliable than the bonding system used in this study.

The dissociation method should be improved since the result of dissociation directly affects the diodicity of the micro valve. Chemical etching or UV laser machining should be tried to dissociate the fixture bridges.

BIBLIOGRAPHY

1. A. B. Frazier. "The Miniaturization Technologies: Past, Present, and Future." *IEEE Transactions on Industrial Electronics,* Vol. 42, No. 5, October 1995, pp. 423.

2. University of Wisconsin- MEMS Laboratory website at: http://mems.engr.wisc.edu/

3. B. K. Paul. "Metal Microlamination for Energy and Chemical Systems Miniaturization." Proposal to ONR's Young Investigator Program (FY 1998), Sept. 1997.

4. C. van Osenbruggen and C. de Regt. "Electrochemical Micromachining." *Philips Tech. Rev,* 42, No. 1, 1985, pp. 22-32.

5. M. Datta. "Microfabrication by through-mask electrochemical micromachining." *SPIE Proceedings,* Vol. 3223, Sep. 29-30, 1997, pp. 178-184.

6. T. Terhaar. "Comparison of Two Microvalve Designs Fabricated in Mild Steel Using Microprojection Welding and Capacitive Dissociation." *Master's Thesis,* Oregon State University, 1998.

7. J. F. Wilson. Practice and Theory of Electrochemical Machining. 1971, pp. 1-19.

8. M. Datta and D. Landolt. "High Rate Transpassive Dissolution of Nickel with Pulsating Current." *Electrochimica Acta,* Vol. 27, No. 3, 1982, pp. 385-390.

9. M. Datta. "Microfabrication by Through-Mask Electrochemical Micromachining." *Proceedings of SPIE, Micromachining and Microfabrication Process Technology III,* Vol. 3223, 1997, pp. 178-184.

10. N. Masuko, T. Osaka and Y. Ito. Electrochemical Technology: Innovation and New Development, 1996, pp.137-157.

11. M. Datta. "Electrochemical Micromachining." *The Electrochemical Society Interface,* Summer 1995, pp. 32-35.

12. American Society for Metals. Metals Handbook, 9th Edition, Vol. 6; Welding, Brazing, and Soldering. 1983, pp. 672-684.

13. American Welding Society. Welding Handbook, 8th Edition, Vol. 2, 1991, pp. 814-818.

14. R. Figliola and D. Beasley. Theory and Design for Mechanical Measurements. 1995, pp. 446-451.

15. D. W. Matson, P. M. Matin, W. D. Bennett, D. C. Stewart, and J. W. Johnston. "Laser micromachined microchannel solvent separator." *SPIE-The International Society for Optical Engineering*. Vol. 3223, September 1997, pp 256.

APPENDICES

APPENDIX A: Procedure for EMM

(A) Making a mask

1. Draw a mask design with the CIM-CAD program.
2. Mount Kaptone (thickness: 125 μm, size: 76.2 mm X 101.6 mm) to a glass slide using rubber cement, then roll with roller.
3. Convert the program file to a laser machine language then expose Kaptone to the laser (repeat design 3 times for 18 hours).
4. Peel off the Kapton from the glass slide. The excess Kapton, etched during EMM processing, will remain on the glass slide.
5. Machined Kapton will have rubber cement residue on backside. Mount the machined using excess rubber cement Kapton to a new glass slide and smooth with roller.

(B) Clean substrate (Stainless Steel 76.2 μm, size: 76.2 mm X 101.6 mm)

1. Degrease the substrate in the hot vapor degreaser (1.1.1. Trichloroethane).
2. Wash the substrate with Micro soap solution.
3. Rinse in DI (deionized) water.
4. Dry with nitrogen.

(C) Spin on AZ 4903 (thick resist: about 4.5 μm) photoresist

Before starting, preheat oven to 90°C. Start vacuum pump.

1. Mount the stainless steel to a glass slide to keep the steel flat.
2. Set spin speed to 3000 rpm. Stop spin.

3. Dispense photoresist onto the backside of the substrate.
4. Start spin cycle. Cycle time = 20 seconds.
5. Bake at 90°C for 30 minutes.
6. Mount the other side (front side) of the stainless steel to a slide.
7. Repeat steps 2 through 5.
8. Remove the stainless steel from the glass slide.

(D) UV (Ultra Violet) Exposure

1. Set the stainless steel and the mask on the "I" line exposure station 365 mm U.V. (upper side: mask, lower side: stainless steel).
2. Expose to UV for 360 seconds with 17.5 mW/cm^2.

(E) Develop the pattern (the stainless steel) in 421 developer

Use 1000cc Pyrex glassware for rinsing and developing beakers.

1. Mix 4 parts developer to 1 part DI water. Usually 200cc developer and 50cc water.
2. Drop substrate into developer and start timer. Agitate. Standard developing time is 75 seconds.
3. Rinse substrate in DI water for 60 seconds.
4. Dry with nitrogen.
5. Inspect substrate with microscope.

(F) Procedure for EMM process

1. Mount the workpiece (the stainless steel with pattern in photoresist) on the lower side of the acrylic fixture with tape.
2. Mount the tool piece, nickel 76.2 μm thick and the same size as a workpiece, on the upper side of the fixing mechanism.
3. Assemble the fixture, set gap between workpiece and toolpiece to 2 mm.
4. Turn on the power of EMM machine, oscilloscope and signal generator.
5. Turn on the power of the electrolyte pump and adjust the temperature of electrolyte to 62°C, then wait for temperature to stabilize.
6. Turn on processing switch, then increase voltage to 20V. 20 Volts is the maximum voltage.
7. Etch time is approximately 2 minutes for 76.2 μm thick 304 stainless steel.
8. After machining, decrease voltage to 0V and turn off the processing switch, then the power of EMM machine.

(G) Cleaning the etched pattern

1. Clean with DI water.
2. Clean with acetone.
3. Degrease in the hot vapor degreaser.

Rinse EMM work area with water to remove salt residue.

APPENDIX B: Pictures

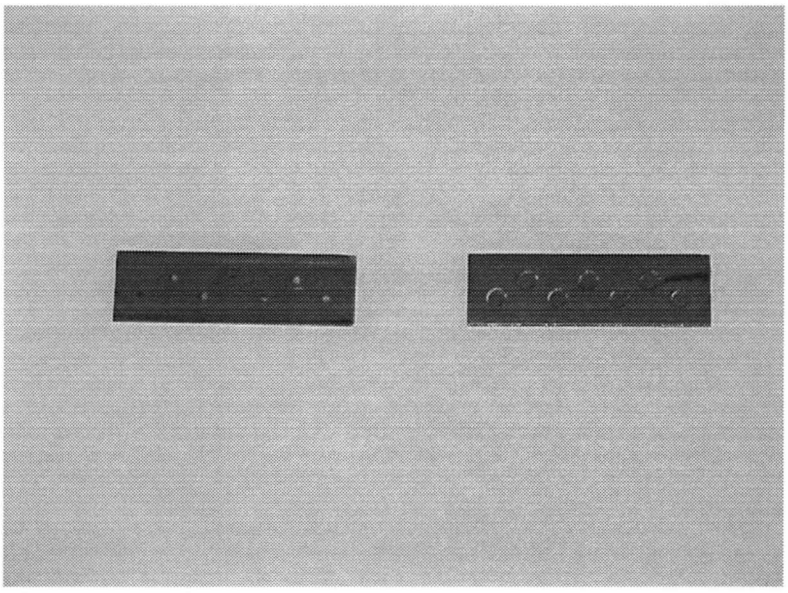

Created Microfloat Valves

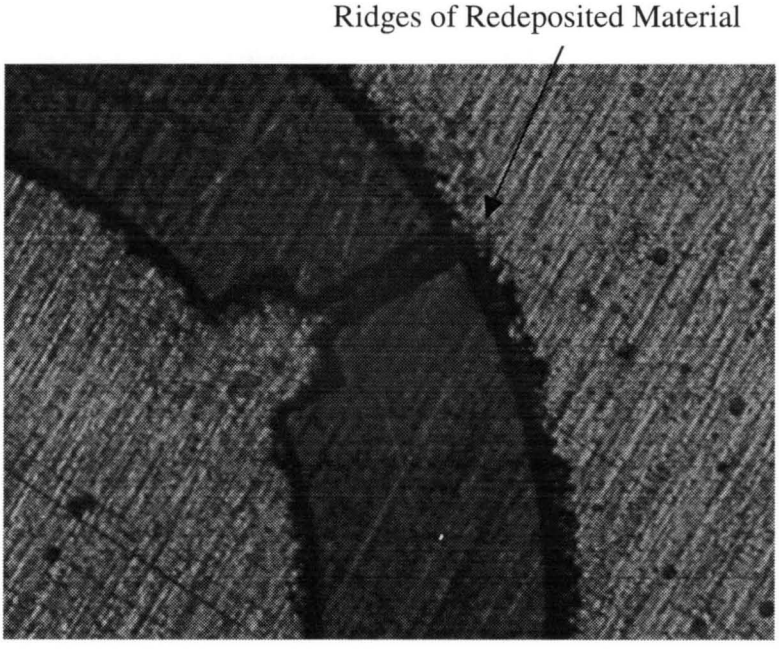

Machined Surface after Laser Ablation

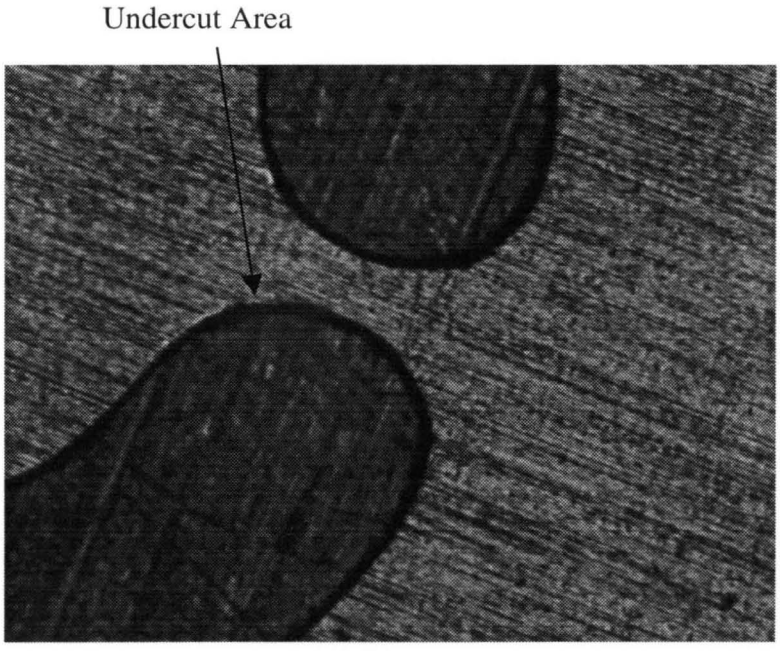

Machined Surface after EMM (Front Side)

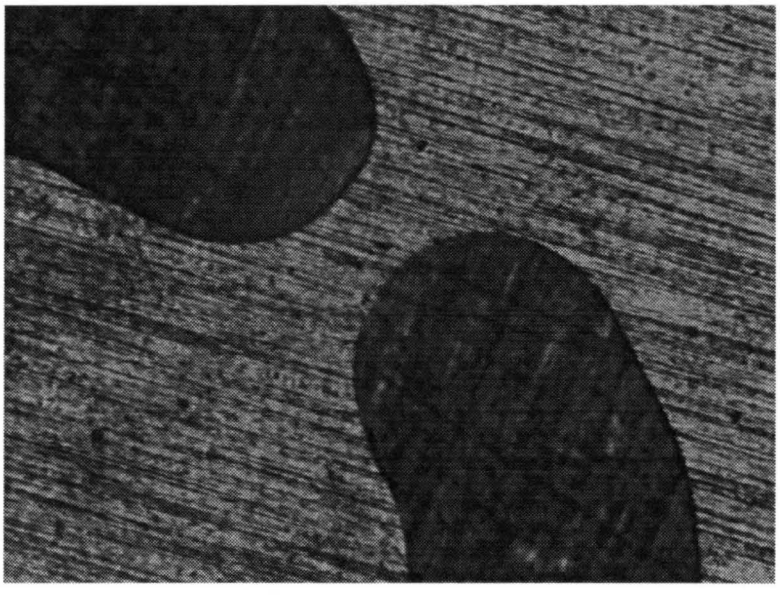

Machined Surface after EMM (Back Side)

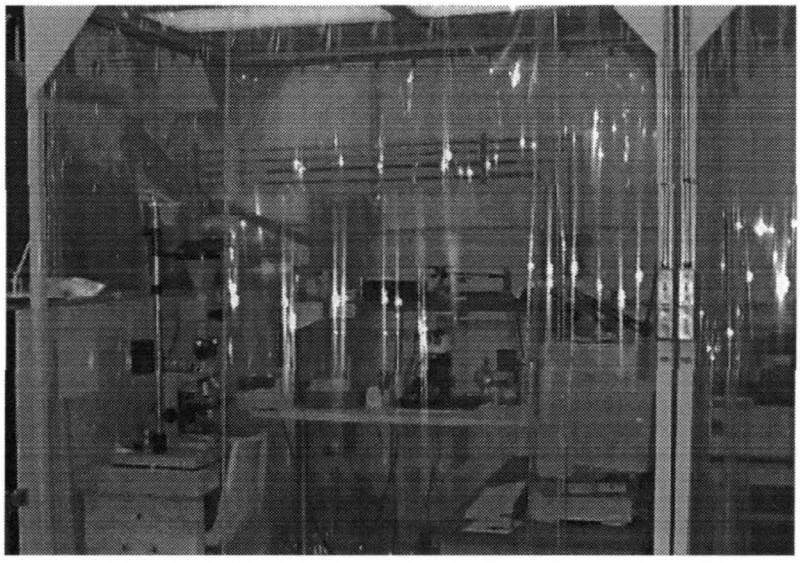

Photolithography Setup

UV Exposure Setup

Potomac LMT-5000 Laser Micromachining System with 12" Stages

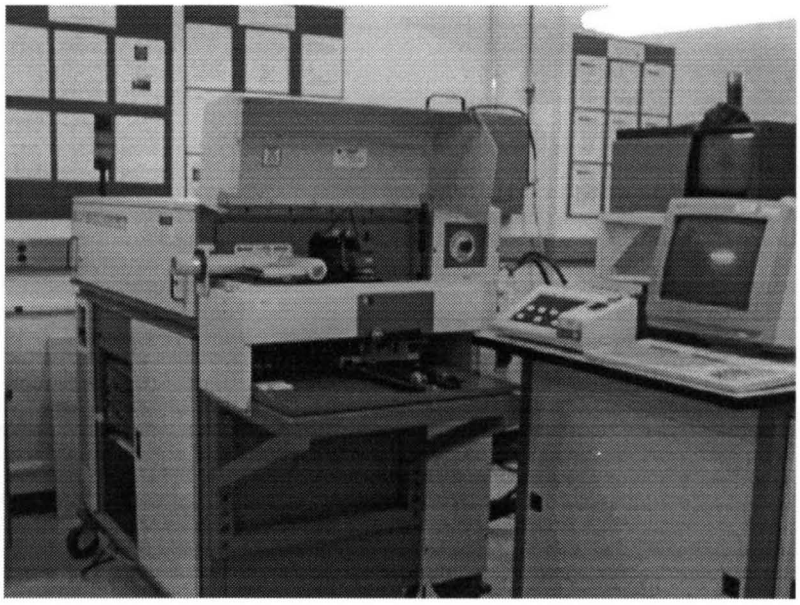

ESI 4420 Laser Machine

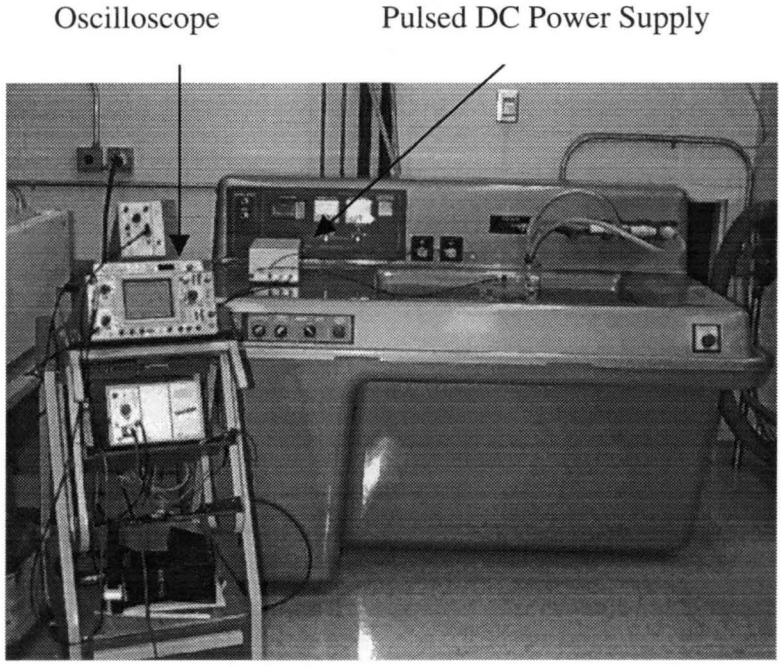

ECX Electrolytic Machining System (EMM Machine)

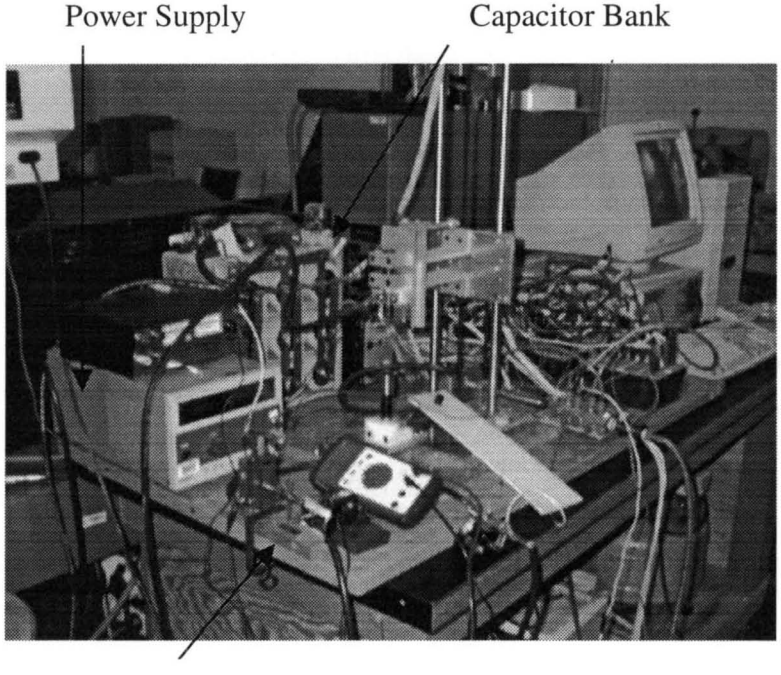

Capacitor Dissociation

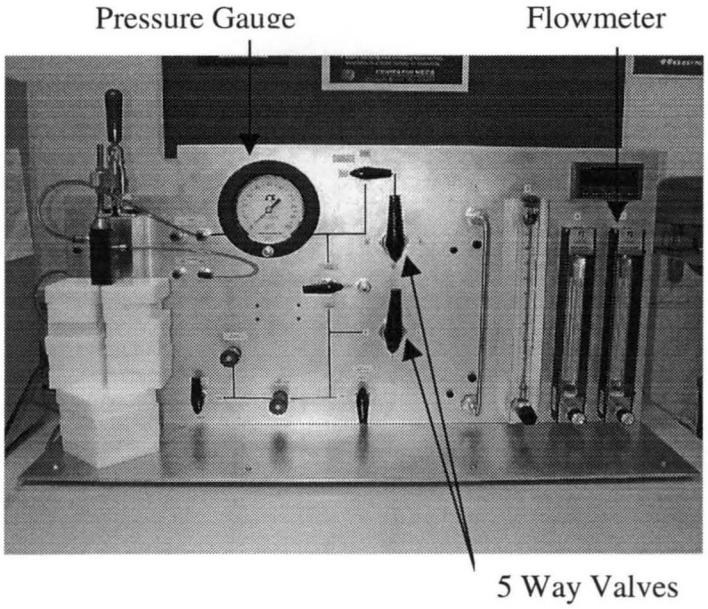

Pressure Test Loop

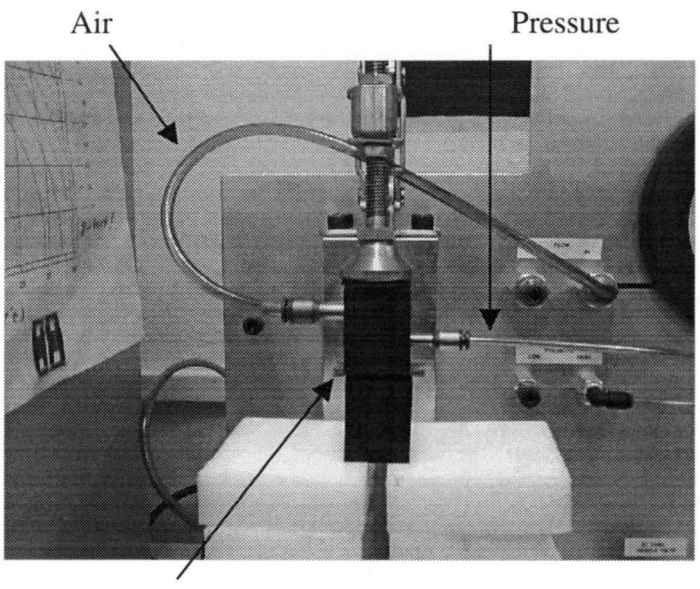

Microfloat Valves Sealed with Gaskets

Fixture for the Test Loop

APPENDIX C: Drawings

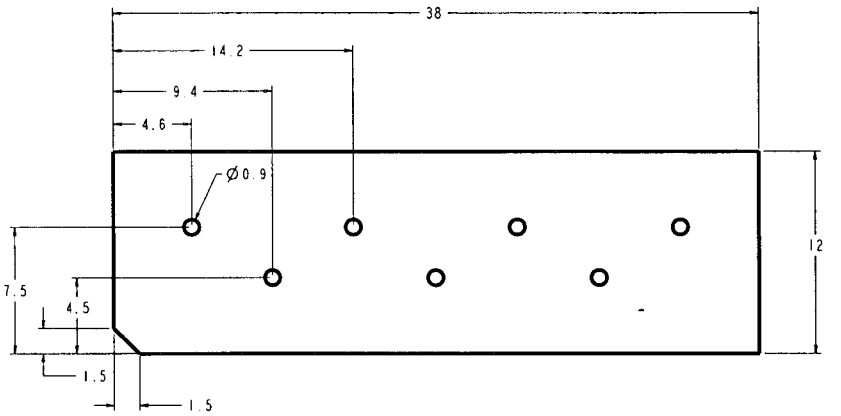

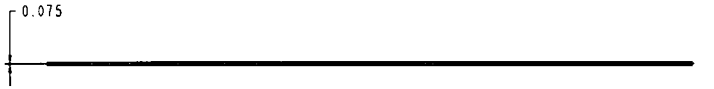

UNLESS OTHERWISE SPECIFIED DIMENSIONS ARE IN MM TOLERANCES ARE:- FRACTIONS ±1/32 DECIMALS .XX ± .01 .XXX ± .005 ANGLES ± 1/2°	CONTRACT NO.		OREGON STATE UNIVERSITY
	APPROVALS	DATE	Laminate I
MATERIAL 304 Stainless Steel	DRAWN Sunghin Park	9/08/99	
	CHECKED		SIZE A / CAGE CODE / DWG NO. Pro-E-1 / REV.
FINISH	ISSUED		
DO NOT SCALE DRAWING			SCALE 10.0 / SHEET 1 of 5

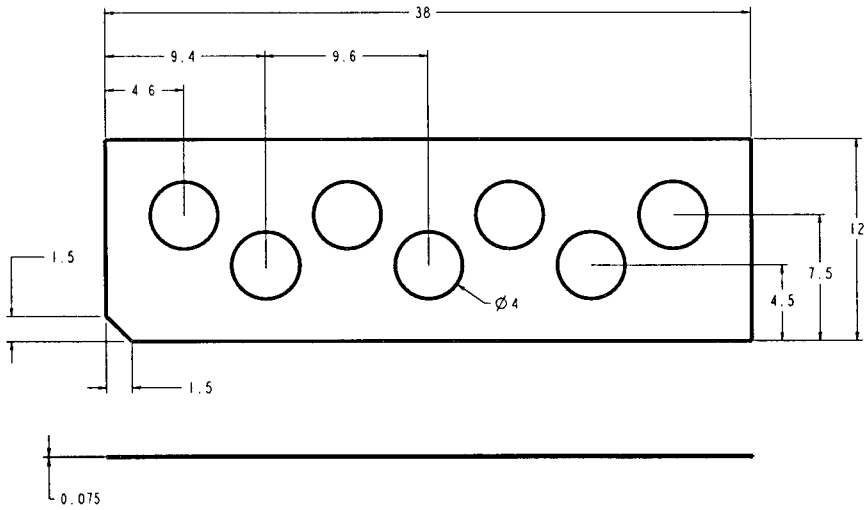

UNLESS OTHERWISE SPECIFIED DIMENSIONS ARE IN MM TOLERANCES ARE: FRACTIONS ±1/32 DECIMALS .XX ± .01 .XXX ± .005 ANGLES ± 1/2°	CONTRACT NO.		OREGON STATE UNIVERSITY
	APPROVALS	DATE	Laminate 2,4,6 and 8
MATERIAL 304 Stainless Steel	DRAWN Songbie Park	9/08/99	
	CHECKED		
FINISH	ISSUED		SIZE A / CAGE CODE / DWG NO. Pro-E-2 / REV.
DO NOT SCALE DRAWING			SCALE 10.0 / SHEET 2 of 5

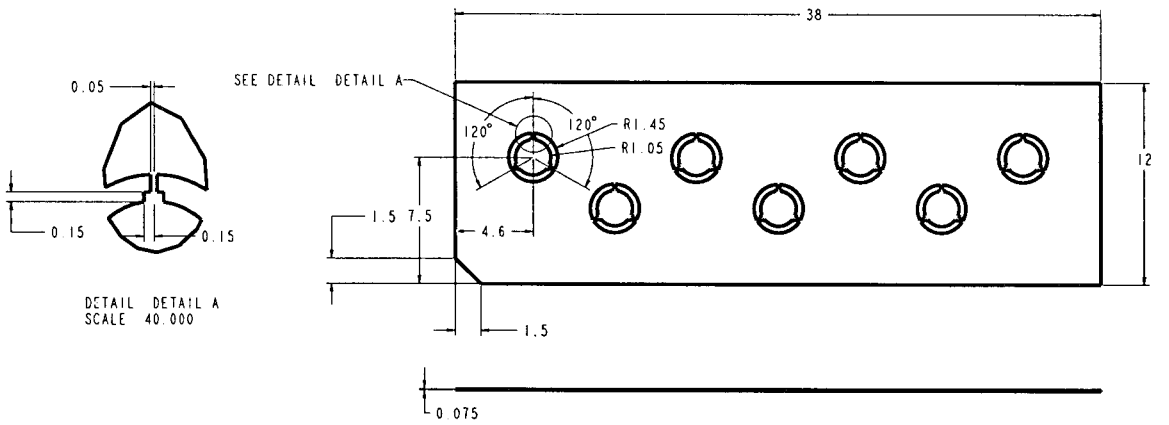

UNLESS OTHERWISE SPECIFIED DIMENSIONS ARE IN MM TOLERANCES ARE: FRACTIONS ±1/32 DECIMALS .XX ± .01 .XXX ± .005 ANGLES ± 1/2°	CONTRACT NO.		OREGON STATE UNIVERSITY
	APPROVALS	DATE	Laminate 3
MATERIAL 304 Stainless Steel	DRAWN Sungbin Park	9/08/99	
	CHECKED		
FINISH	ISSUED		SIZE A / CAGE CODE / DWG NO. Pro-E-3 / REV.
DO NOT SCALE DRAWING			SCALE 10.0 / SHEET 3 of 5

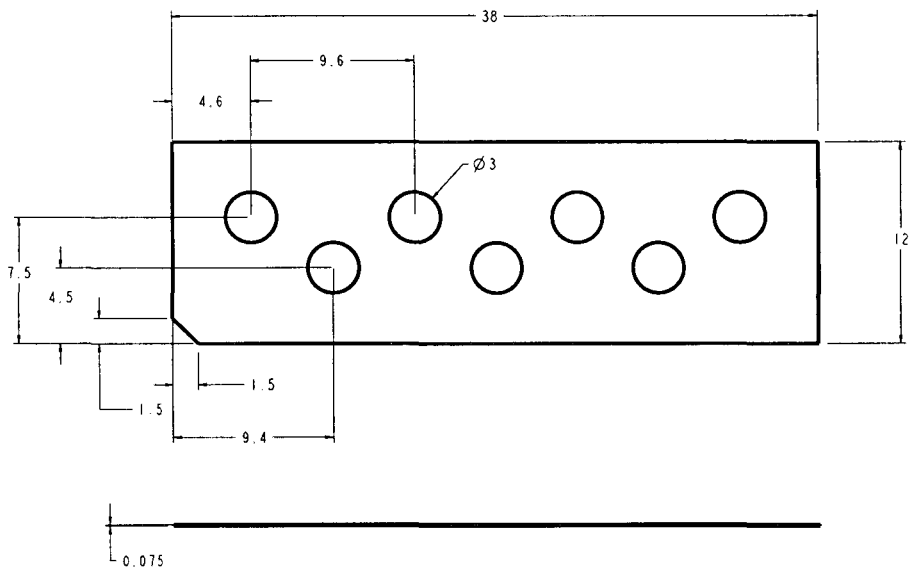

UNLESS OTHERWISE SPECIFIED DIMENSIONS ARE IN MM TOLERANCES ARE: FRACTIONS ±1/32 DECIMALS .XX ± .01 .XXX ± .005 ANGLES ± 1/2°	CONTRACT NO.		OREGON STATE UNIVERSITY
	APPROVALS	DATE	Laminate 5 and 7
MATERIAL 304 Stainless Steel	DRAWN Songbin Park	9/08/99	
	CHECKED		
FINISH	ISSUED		SIZE A / CAGE CODE / DWG NO. Pre-E-4 / REV.
DO NOT SCALE DRAWING			SCALE 10.0 / SHEET 4 of 5

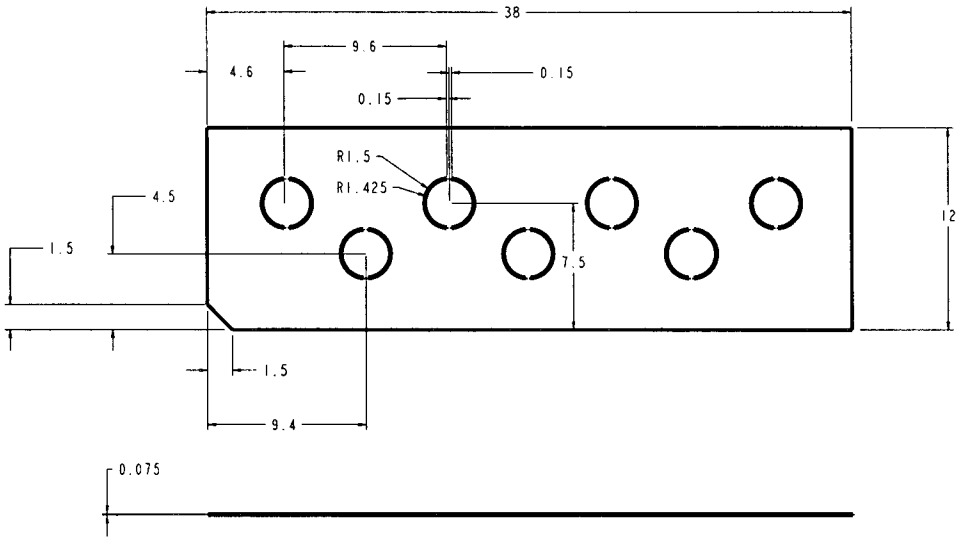

UNLESS OTHERWISE SPECIFIED DIMENSIONS ARE IN MM TOLERANCES ARE:- FRACTIONS ±1/32 DECIMALS .XX ± .01 .XXX ± .005 ANGLES ± 1/2°	CONTRACT NO.		OREGON STATE UNIVERSITY
	APPROVALS	DATE	Laminate 9
MATERIAL 304 Stainless Steel	DRAWN Seaghin Park	9/08/99	
	CHECKED		
FINISH	ISSUED		SIZE A / CAGE CODE / DWG NO. Pro-E-5 / REV.
DO NOT SCALE DRAWING			SCALE 10.0 / SHEET 5 of 5

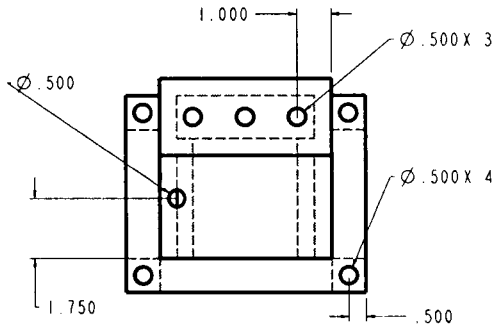

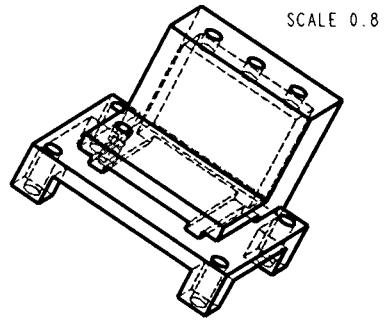

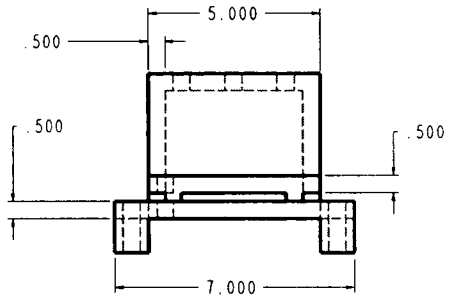

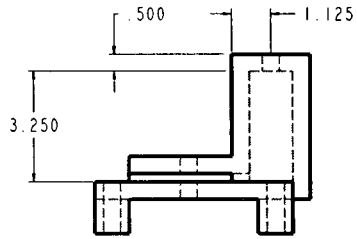

UNLESS OTHERWISE SPECIFIED DIMENSIONS ARE IN INCHES TOLERANCES ARE: FRACTIONS ±1/32 DECIMALS .XX ± .01 XXX ± .005 ANGLES ± 1/2°	CONTRACT NO.		OREGON STATE UNIVERSITY
	APPROVALS	DATE	
MATERIAL ACRYLIC SHEET	DRAWN Sang-Bin Park	10/27/99	Fixture for EMM
	CHECKED		
FINISH	ISSUED		SIZE A / CAGE CODE / DWG NO. Pro-E-6 / REV
DO NOT SCALE DRAWING			SCALE 0.8 / SHEET 1 of 1